Systematic revision and redefinition of the genus *Scirrotherium* Edmund and Theodor, 1997 (Cingulata, Pampatheriidae): Implications for the origin of pampatheriids and the evolution of the South American lineage including *Holmesina*

Kevin Jiménez-Lara [a, b]

[a] División de Paleontología de Vertebrados, Museo de La Plata, Facultad de Ciencias Naturales y Museo, Universidad Nacional de La Plata, Paseo del Bosque s/n, B1900FWA La Plata, Argentina.

[b] CONICET, Consejo Nacional de Investigaciones Científicas y Técnicas, Argentina.

e-mail: kjimenezlara@fcnym.unlp.edu.ar

Abstract

The intrageneric relationships of the pampatheriid genus *Scirrotherium* and its affinities with supposedly related genera, i.e., *Kraglievichia* and *Holmesina*, are revised through parsimony phylogenetic analyses and new comparative morphological descriptions. For this work, unpublished material of pampatheriids (numerous osteoderms, one partial skull and a few postcranial bones) from Neogene formations of Colombia was analyzed. The results show that *Scirrotherium* is paraphyletic if we include all its referred species, i.e., *Scirrotherium hondaensis*, *S. carinatum* and *S. antelucanus*. The species *S. carinatum* is closer to *Kraglievichia paranensis* than to *S. hondaensis* or *S. antelucanus*, therefore the

new name *K. carinatum* comb. nov. is proposed. The relationship among *S. hondaensis* and *S. antelucanus* could not be resolved, so these species should be designated in aphyly. In spite of failing to recover *S. hondaensis* and *S. antelucanus* as one single clade, here is preferred to maintain the generic name *Scirrotherium* in both species based on diagnostic evidence. New emended diagnoses for *Scirrotherium*, *S. hondaensis* and *Kraglievichia* are provided. The genus *Holmesina* was found to be monophyletic and positioned as the sister clade of *Scirrotherium* + *Kraglievichia*. The evolutionary and biogeographic implications of the new phylogeny and taxonomic re-arrangements are discussed. A possible geographic origin of the family Pampatheriidae and *Scirrotherium* in low latitudes of South America as early as Early Miocene times is claimed. The South American ancestor or sister taxon of *Holmesina* is predicted to be morphologically more similar to *Scirrotherium* than to *Kraglievichia*.

Keywords: Pampatheriidae

Scirrotherium

Kraglievichia

Holmesina

Great American Biotic Interchange

Neogene

1. Introduction

The pampatheriids (Pampatheriidae) are a morphologically conservative extinct clade of glyptodontoid cingulates (Xenarthra: Glyptodontoidea *sensu* McKenna and Bell 1997) with medium-to-large body sizes (Edmund 1985; Góis et al. 2013). They were distributed from the Neogene to the Early Holocene in numerous localities in South America (their native range), Central America, Mexico and the United States (Edmund 1985; Vizcaíno et al. 1998; Rincón et al. 2014; Góis et al. 2015 and references therein). As the modern armadillos (Dasypodidae), pampatheriids have a flexible carapace characterized by the presence of three transverse bands of imbricated osteoderms, which form a kind of "articulation" between the scapular and pelvic shields (Edmund 1985). The pampatheriids also have multiple features, especially in their skull and mandible, which, collectively, define them as the sister group of glyptodontids –Glyptodontidae (Gaudin 2004; Gaudin and Wible 2006; Billet et al. 2011; Delsuc et al. 2012), namely, a deep horizontal mandibular ramus, a laterally-directed zygomatic root, a transversely wide glenoid fossa, rugose pterygoids, among others (Gaudin and Wible, 2006).

The fossil record of Pampatheriidae is mainly represented by isolated specimens, most of which are osteoderms and, to a lesser extent, skulls, mandibles and postcranial bones. Relatively complete and articulated skeletons are uncommon (Edmund 1985; Góis 2013). Due to this fact, the systematics of this group has historically been based on osteoderm characters (Edmund 1985, 1987; Góis et al. 2013), as has often been the case with other cingulate clades. Overall, nearly 20 pampatheriid species and seven genera are known (Góis 2013). The latter conform two possible subfamilial lineages: (1) that including to the genera *Plaina* and *Pampatherium*; and (2) that comprising the genera *Scirrotherium*, *Kraglievichia* and *Holmesina* (Edmund 1985). However, there is no any published

65 phylogenetic analysis on the relationships among the different pampatheriid genera in the
66 scientific literature. Only Góis (2013) performed a phylogenetic analysis of these taxa, but
67 his results have not been published so far. In Góis's consensus tree, it was corroborated the
68 hypothesis on the two subfamilial lineages as suggested by Edmund (1985).

69 The genus *Scirrotherium* is the oldest undoubted pampatheriid (Góis et al. 2013; Rincón et
70 al. 2014) and one of the four Miocene genera (the others are *Kraglievichia* Castellanos
71 1927; *Vassallia* Castellanos, 1927; and *Plaina* Castellanos, 1937). This taxon was
72 originally described by Edmund and Theodor (1997) based on craniomandibular,
73 postcranial and osteoderm specimens collected in the Middle Miocene (Serravalian)
74 sedimentary sequence of the La Venta area, in southwestern Colombia. These authors
75 suggested that the type and only known species in that time, *Scirrotherium hondaensis*, has
76 plesiomorphic traits in its osteological morphology which are expected for its antiquity.
77 Additionally, they highlighted the morphological similarity of *S. hondaensis* with the
78 species *Vassallia minuta* (Late Miocene of southern and central South America; De Iullis
79 and Edmund 2002), more than with any other pampatheriid.

80 Later, Góis et al. (2013) described a second species for *Scirrotherium*, *S. carinatum*, from
81 the Late Miocene (Tortonian) of northeastern and southern Argentina and northwestern
82 Brazil. In northeastern Argentina (Province of Entre Ríos), *S. carinatum* is found in the
83 same basal stratigraphic levels ("Conglomerado Osífero", literally meaning 'bone-bearing
84 conglomerate') of the Ituzaingó Formation as the middle-sized pampatheriid *Kraglievichia*
85 *paranensis* (Góis et al. 2013; Scillato-Yané et al. 2013), a taxon clearly distinct but not
86 distantly related to *Scirrotherium*, as previously indicated. *Scirrotherium carinatum*, based

87 exclusively on osteoderms from different regions of the armored carapace, has an estimated
88 body size comparable or slightly smaller than that of *S. hondaensis* (Góis et al. 2013).

89 The phylogenetic analysis conducted by Góis (2013) recovered a polytomy involving *S.*
90 *carinatum* and *S. hondaensis*, one of these species or both being the sister taxon/taxa of the
91 clade *Kraglievichia* + *Holmesina* (except *H. floridanus*). Considering that *Scirrotherium* is
92 the oldest known pampatheriid, it is notorious the non-basal position of the *Scirrotherium*
93 species in the cladogram of Góis (2013). Instead, these species are closely allied with
94 terminal taxa, i.e., *Holmesina* spp. (Edmund 1985, 1987; Gaudin and Lyon 2017). If this
95 result is correct, it would indicate a significant ghost lineage at the base of Pampatheriidae.

96 Góis (2013) found phylogenetic support for *Scirrotherium* through one single
97 synapomorphy, i.e., the presence of deep longitudinal depressions in the osteoderms. This
98 is a distinctive feature of *S. carinatum* but the longitudinal depressions in *S. hondaensis* are
99 relatively shallow. Interestingly, this putative synapomorphy is actually shared by *K.*
100 *paranensis*. Góis (2013) explained the lack of phylogenetic resolution for *Scirrotherium* by
101 noting the fragmentary character of the available fossil specimens of *S. hondaensis*.
102 However, unlike the latter species, the skull, mandible and any postcranial bone of *S.*
103 *carinatum* are unknown (Góis et al. 2013).

104 Laurito and Valerio (2013) reported new pampatheriid material from the Late Miocene
105 (Tortonian to Messinian) of Costa Rica, which they assigned to a new species, *S.*
106 *antelucanus*. This species, the largest referred to as *Scirrotherium* so far (body size
107 comparable or slightly smaller than that of *K. paranensis*; Laurito and Valerio 2013), is
108 based on osteoderms and some postcranial bones (femoral fragments and metatarsals). The
109 occurrence of *S. antelucanus* in the Late Miocene of southern Central America suggests

that *Scirrotherium* took part in the late Cenozoic biotic interchanges of the Americas earlier than any other pampatheriid (i.e., *Plaina*, *Pampatherium*, *Holmesina*; Woodburne 2010), invading tropical North America ("North America" is defined here as all the continental territories north of the ancient location of the main geographic barrier between the Americas during the early Neogene, i.e., the Central American Seaway in northwestern Colombia) before the definitive closing of the Panamanian Land Bridge (PLB) ca. 3 mya (Schmidt 2007; Coates and Stallard 2013; O'dea et al. 2016; Jaramillo 2018).

Recently, the occurrence of isolated osteoderms designated as *Scirrotherium* sp. or cf. *Scirrotherium* has been reported in several contributions on fossil vertebrate assemblages from the Neogene of Venezuela and Peru. On the basis of these discoveries, the geographic and chronological distribution of the genus has been expanded in such a way that this taxon is now known for the Early and Late Miocene (Burdigalian and Tortonian) of northwestern Venezuela (Rincón et al. 2014; Carrillo-Briceño et al. 2018) and Late Miocene (Tortonian) of eastern Peru (Antoine et al. 2016).

Assuming all the previous taxonomic assignments are correct, the latitudinal range of *Scirrotherium*, from southern Central America to Patagonia (southern Argentina), is the widest latitudinal range of a Miocene pampatheriid, comparable only with those of the Plio-Pleistocene forms *Pampatherium* and *Holmesina* (Scillato-Yané et al. 2005). This biogeographic evidence provides support for the hypothesis that *Scirrotherium* inhabited varied environments within its latitudinal range, and, consequently, that it probably had a relatively high ecological flexibility (Góis et al. 2013).

Despite the progress in the systematic and biogeographic research on *Scirrotherium*, a new reevaluation of several fundamental hypotheses about this taxon is needed, including its

taxonomic definition and evolutionary relationships with other pampatheriid genera. Using parsimony phylogenetic analyses and comparative morphological descriptions of new pampatheriid remains from the Neogene of Colombia, this contribution reevaluates the taxonomic status of *Scirrotherium* and its relationships with supposedly allied genera, i.e., *Kraglievichia* and *Holmesina*. Accordingly, I suggest a new taxonomic and nomenclatural reorganization, with emended diagnoses for *Scirrotherium* and *Kraglievichia*.

Finally, considering the systematic reanalysis, I develop a model of biogeographic evolution for the lineage *Scirrotherium-Kraglievichia-Holmesina*. From this model, I draw out new hypotheses on the geographic origin of Pampatheriidae and the late Cenozoic dispersal events of pampatheriids to/from North America, including a possible re-entry event to South America for the species *S. antelucanus*.

2. Material and methods

2.1. Taxonomic sampling

I studied 12 species of pampatheriids attributed to six different genera. These species, in alphabetic order, are: *Holmesina floridanus* Robertson, 1976; *H. major* Lund, 1842; *H. occidentalis* Hoffstetter, 1952; *H. paulacoutoi* Cartelle and Bohórquez, 1985; *H. septentrionalis* Leidy, 1889; *Kraglievichia paranensis* Ameghino, 1888; *Pampatherium humboldtii* Lund, 1839; *Plaina intermedia* Ameghino, 1888; *Scirrotherium antelucanus* Laurito and Valerio, 2013; *S. carinatum* Góis, Scillato-Yané, Carlini and Guilherme, 2013; *S. hondaensis* Edmund and Theodor, 1997; and *Vassallia minuta* Moreno and Mercerat, 1891. Unidentified pampatheriid material (MUN STRI 16718 and 38064; see the section

155 *Institutional abbreviations*) from the Castilletes Formation in Colombia (see below), which
156 is referred to as "Castilletes specimens", was also included in this selection.

157 Among the former nominal species, I follow Góis (2013) in considering *Vassallia maxima*
158 as a junior synonym of *Pl. intermedia*. The only species of *Holmesina* not included in this
159 study were *H. rondoniensis* Góis, Scillato-Yané, Carlini and Ubilla, 2012 and *H. cryptae*
160 Moura, Góis, Galliari and Fernandes 2019. In the case of *H. rondoniensis*, its exclusion is
161 based on a preliminary phylogenetic analysis in which it was identified as a "wildcard"
162 taxon obscuring phylogenetic resolution as a result of lack of information on the osteoderm
163 features of this species. On the other hand, the scientific article in which *H. cryptae* was
164 described has been very recently published (Moura et al. 2019), after the completion of this
165 work. Consequently, it was preferred to omit this species here. *Tonnicinctus mirus* Góis,
166 González Ruiz, Scillato-Yané and Soibelzon, 2015 was also not included in this analysis
167 given that this species is considered a highly divergent taxon without any apparent
168 substantial interest with respect to the systematic issues here addressed.

169

170 *2.2. Morphological description of the specimens*

171 The osteological morphology of the selected species was re-examined from direct
172 observations of specimens and published/unpublished descriptions (Simpson 1930,
173 Castellanos 1937; Edmund 1985, 1987; Edmund and Theodor 1997; Góis 2013; Góis et al.
174 2013; Laurito and Valerio 2013; Scillato-Yané et al. 2013; Góis et al. 2015; Gaudin andg
175 Lyon 2017). Naturally, according to the objectives of this research, during the revision of
176 material I focused on the species *S. antelucanus*, *S. carinatum* and *S. hondaensis*, and,

177 additionally, species of genera considered closely allied to *Scirrotherium*, i.e., *K.*
178 *paranensis* and *Holmesina* spp. (particularly *H. floridanus*; Appendix S1 of the
179 Supplementary Material).

180 On the other hand, new undescribed cranial, postcranial and osteoderm specimens were
181 also used to reevaluate the morphological variability of *Scirrotherium*. This material comes
182 from five Neogene geological units of Colombia (Fig. 1): (1) Castilletes Formation (Early
183 to Middle Miocene, late Burdigalian-Langhian), Municipality of Uribia, Department of La
184 Guajira; (2) La Victoria Formation (late Middle Miocene, Serravalian), Municipality of
185 Villavieja, Department of Huila; (3) Villavieja Formation (late Middle Miocene,
186 Serravalian), Municipality of Villavieja, Department of Huila; (4) Sincelejo Formation
187 (Late Miocene-Early Pliocene, Messinian-Zanclean), Municipality of Los Palmitos,
188 Department of Sucre; (5) Ware Formation (Late Pliocene, Piacenzian), Municipality of
189 Uribia, Department of La Guajira. For detailed lithological descriptions and
190 chronostratigraphic data on these formations, the reader is referred to the following
191 references: Moreno et al. (2015) for the Castilletes and Ware Formations; Guerrero (1997),
192 Flynn et al. (1997) and Anderson et al. (2016) for the La Victoria and Villavieja
193 formations; and Flinch (2003), Villarroel and Clavijo (2005), Bermúdez et al. (2009) and
194 Alfaro and Holz (2014) for the Sincelejo Formation. The new fossils are deposited in the
195 Paleontological Collection of the Museo Mapuka de la Universidad del Norte, Barranquilla,
196 Colombia, except those collected in the La Victoria and Villavieja Formations. The latter
197 are housed at the Museo de Historia Natural La Tatacoa, La Victoria Town, Municipality of
198 Villavieja, Department of Huila, Colombia.

Cranial measurements, all taken on the midline of the skull (dorsally or ventrally), follow Góis (2013). The anatomical terminology for osteoderms is based on the proposals by Góis et al. (2013). All the measurements were taken with a digital caliper.

2.3. Character matrix

I used exclusively cranial, dental and osteoderm characters, given that postcranial bones of most species of Pampatheriidae are poorly known (Góis 2013). The character construction was based on personal observations and previous quantitative and qualitative analyses of the interspecific, intergeneric and familial morphological variability of pampatheriids (e.g., Edmund 1985, 1987; Góis 2013; Góis et al. 2013; Laurito and Valerio 2013; Gaudin and Lyon, 2017). Overall, a matrix of 27 characters (Appendix S2 of the Supplementary Material) was built and managed on Mesquite version 2.75 (Maddison and Maddison 2010). If present, parsimony-uninformative characters were used to define potential autapomorphies of the taxa under study.

2.4. Cladistic analyses

Parsimony analyses under schemes of equal weights and implied weights (characters reweighted *a posteriori*; see below) were performed in PAUP* version 4.0a142 (Swofford 2015). In both weighting schemes, the species *P. humboldtii*, *Pl. intermedia* and *V. minuta* were selected as outgroup (sister group). This selection is based on the hypothesis about subfamilial relationships of Pampatheriidae by Edmund (1985) and the phylogeny of Góis (2013). All the characters were treated as unordered. The analyses were run with the branch

and bound search to estimate maximum parsimony trees. The criterion for character optimization was DELTRAN (see Gaudin [2004] for justification of this configuration). For reordering of branches, the algorithm of tree-bisection-reconnection (TBR) branch swapping was used. The topological results of most parsimonious trees were summarized through strict consensus trees.

In this work, the methodology of implied weights was intended to mitigate potential biases arising from limited number of characters (especially osteoderm characters, as a consequence of the evolutionary trend in Pampatheriidae towards a simplification of the ornamentation in comparison with that in other cingulate clades, e.g., Glyptodontidae) and the effect of homoplastic characters (Goloboff et al. 2008; Goloboff 2014). Characters were reweighted using the rescaled consistency index (mean value) of the equally-weighted parsimony analysis (see Ausich et al. 2015 and references therein for justification of the use of rescaled consistency index for implied-weights parsimony analyses). A default concavity value (k = 3) was selected (Goloboff et al. 2018). Three successive rounds of character reweighting were needed until identical set of strict consensus trees were found in two consecutive searches (Swofford and Bell 2017).

Node stability for the strict consensus trees was evaluated using bootstrap resampling procedures (branch and bound search with 100 replicates). The software FigTree v1.4.3 (http://tree.bio.ed.ac.uk/software/figtree/) was used as a graphical viewer and editor for the cladograms.

2.5. Taxonomic and nomenclatural criteria

I applied a taxonomic and nomenclatural criterion reasonably, but not strictly, constrained by the phylogeny. This implies looking for a natural classification (i.e., based on monophyletic groups) without ignoring possible limitations of the phylogenetic inference related to the available information in the fossil record and major morphological gaps. Additionally, open nomenclature was used to indicate taxonomic uncertainty when necessary, following the general recommendations of Bengston (1988) and updated definitions by Sigovini et al. (2016) for the qualifiers of this semantic tool of taxonomy.

2.6. Institutional abbreviations

CFM, Museo Nacional de Costa Rica, Colección de fósiles de la sección de Geología, San José, Costa Rica; FMNH, Field Museum Natural History, Chicago, Illinois, USA; MACN, Museo Argentino de Ciencias Naturales "Bernardino Rivadavia", Colección de Paleovertebrados, Ciudad Autónoma de Buenos Aires, Argentina; MCL, Museu de Ciências Naturais da Pontifícia Universidade Católica de Minas Gerais, Belo Horizonte, Brazil; MG-PV, Museo Provincial de Ciencias Naturales Dr. Ángel Gallardo, Rosario, Argentina; MHD-P, Museo Histórico Departamental de Artigas, Artigas, Uruguay; MLP, Museo de La Plata, La Plata, Argentina; MUN STRI, Museo Mapuka de la Universidad del Norte, Colección de paleontología, Barranquilla, Colombia; ROM, Royal Ontario Museum, Toronto, Canadá; UCMP, University of California Museum of Paleontology, Berkeley, California, USA; UF, Florida Museum of Natural History, Gainesville, Florida, USA; UZM, Universitets Zoologisk Museum, Copenhagen, Denmark; VPPLT, Museo de Historia Natural La Tatacoa, Colección de paleontología, La Victoria Town, Huila, Colombia.

2.7. Anatomical abbreviations

FL, frontal bone length; GFL, greatest femoral length; GSL, greatest skull length; LUR, length of the upper teeth row; Mf, upper molariform; mf, lower molariform; NL, nasal bone length; PAL, parietal bone length; PL, hard palate length; TTW, maximum width at the third trochanter of the femur; DW, maximum width of the femoral distal epiphysis.

3. Results

The parsimony analysis with equal weights obtained 107 most parsimonious trees (MPTs), each one of these with a tree length of 44 steps (consistency index = 0.909; retention index = 0.907; rescaled consistency index = 0.825). The strict consensus tree from these MPTs (Fig. 2 (A); tree length = 52; consistency index = 0.769; retention index = 0.721; rescaled consistency index = 0.555) is not fully resolved because it has two polytomies. One of these polytomies involves the species *S. hondaensis*, *S. antelucanus* and *H. floridanus*, whereas the other is formed by *H. septentrionalis*, *H. major*, *H. paulacoutoi* and *H. occidentalis*. Three clades were recovered (excluding that of the entire ingroup): (1) All the ingroup taxa except "Castilletes specimens"; (2) *S. carinatum* + *K. paranensis*; and (3) *Holmesina* spp. except *H. floridanus*. On the other hand, the parsimony analysis with implied weights yielded 30 most parsimonious trees (MPTs) with a tree length of 109 weighted steps (consistency index = 0.982; retention index = 0.982; rescaled consistency index = 0.964). The strict consensus tree from the MPTs (Fig. 2(B); tree length = 91; consistency index = 0.978; retention index = 0.980; rescaled consistency index = 0.959), like that produced by

the equally weighted approach, is not fully resolved. Again, two polytomies resulted, but in this case the polytomy including *S. hondaensis*, *S. antelucanus* and *H. floridanus* was altered. The latter taxon was placed as the basal-most *Holmesina* species. The polytomy formed by *H. septentrionalis*, *H. major*, *H. paulacoutoi* and *H. occidentalis* was unmodified. As a consequence of the relocation of *H. floridanus* within the topology, four clades were recovered: (1) All the ingroup taxa except "Castilletes specimens"; (2) *S. carinatum* + *K. paranensis*; (3) *Holmesina* spp.; and (4) *H. septentrionalis*, *H. major* + *H. paulacoutoi* + *H. occidentalis*. According to the two schemes of weighting for the parsimony analyses, *Scirrotherium* is paraphyletic if it is comprised of *S. antelucanus*, *S. hondaensis* and *S. carinatum*. *Scirrotherium carinatum* is closer to *K. paranensis* than to *S. hondaensis* or *S. antelucanus*. The relationship among *S. hondaensis* and *S. antelucanus* is not resolved in either of the two strict consensus trees.

Under the equal weights analysis, all the nodes that include taxa of interest show (nearly) significant stability (resampling frequencies ca. 70 or greater). As expected, a similar result was obtained in the bootstrap resampling under implied weights, but with improved frequencies for nearly all the branches (except the basal-most branch, whose frequency decreased slightly from that of the former bootstrapping [85 to 83]).

4. Systematic paleontology

Xenarthra Cope, 1889

Cingulata Illiger, 1811

Glyptodontoidea Gray, 1869

Pampatheriidae Paula Couto, 1954

Scirrotherium Edmund and Theodor, 1997

LSID. urn:lsid:zoobank.org:act:313358B5-3B1F-4902-8C2E-BB07CFCBEE18

Type species: *Scirrotherium hondaensis* Edmund and Theodor, 1997 by original designation.

Emended diagnosis: A pampatheriid of small-to-middle body size that can be distinguished from other pampatheriids by the following combination of features: thin non-marginal fixed osteoderms (ca. 3.5–7 mm in thickness); slightly to moderately rough external surface of osteoderms; external surface of osteoderms with a sharp and uniformly narrow longitudinal central elevation; longitudinal central elevation from superficial to well-elevated; (very) shallow longitudinal depressions with gentle slope towards the marginal elevations; usually one single, transversely elongated row of large foramina in the anterior margin of fixed osteoderms; maximum number of foramina per row between 6 and 11.

Remarks: The taxonomic status of *Scirrotherium* is saved from invalidity by paraphyly by exclusion of the species '*S.*' *carinatum* from the genus (see below). However, according to the preferred phylogenetic hypothesis presented here, i.e., the strict consensus tree from the parsimony analysis under implied weights (Fig. 2(B)), the other two referred species of *Scirrotherium*, *S. antelucanus* and *S. hondaensis*, should be designated in aphyly because they do not have resolved relationship between them (see Ebach and Williams 2010 for details about the phylogenetic concept of aphyly). Until new evidence becomes available, maintenance of the taxonomic validity of *Scirrotherium*, as defined here, is based on the

emended diagnosis of this taxon, which is partially built from ambiguous synapomorphies, as well as from qualitative and quantitative morphological differences with other genera.

Scirrotherium hondaensis Edmund and Theodor, 1997

LSID. urn:lsid:zoobank.org:act:E3B83181-91D6-44C8-90C0-BBAACEC2CDEE

Holotype: UCMP 40201, incomplete skull and left hemimandible (Edmund and Theodor, 1997).

Type locality and horizon: Municipality of Villavieja, Department of Huila, Colombia. La Victoria Formation, upper Middle Miocene, Serravalian (Edmund and Theodor, 1997).

Emended differential diagnosis. Pampatheriid of small body size that differs from other pampatheriids based on this unique combination of characters: external surface of osteoderms with ornamentation (especially the longitudinal central elevation and marginal elevations), in general terms, more protuberant than in *S. antelucanus*, but less than in *Kraglievichia*; size range of fixed osteoderms smaller than in *S. antelucanus* and similar to that in *Kraglievichia carinatum* comb. nov. (= '*S.*' *carinatum*; Góis et al. 2013; see below); fixed osteoderms generally thicker than in *K. carinatum* comb. nov. but less than in *K. paranensis*, similar to *S. antelucanus*; anterior foramina smaller than in *S. antelucanus*; anterior foramina in fixed osteoderms usually aligned in one individual row, although infrequently these osteoderms show an extra, short or reduced row of anterior foramina; two rows of anterior foramina in mobile osteoderms, similar to *Vassallia* (Góis 2013); mf9 incipiently bilobed; frontals prominently convex in lateral view, with this convexity

352 positioned posterior to the insertion of the anterior root of the zygomatic arch; anterior root
353 of the zygomatic arch posterolaterally projected with respect to the main body of maxilla.

354 **Referred material**: VPPLT 004, several fixed osteoderms; VPPLT 264, several fixed
355 osteoderms and one semi-mobile osteoderm; VPPLT 348, tens of fixed and (semi) mobile
356 osteoderms; VPPLT 701, several fixed osteoderms; VPPLT 706, one anterior skull, one
357 femoral diaphysis, one ulna without distal epiphysis, several vertebrae and numerous fixed
358 and (semi) mobile osteoderms; VPPLT 1683 - MT 18, several fixed and (semi) mobile
359 osteoderms; UCMP 39846, one proximal femoral epiphysis, one left calcaneum and one
360 left astragalus. All the osteoderms referred to as *S. hondaensis* are illustrated in Fig. 3.
361 Other important specimens are illustrated in Figs. 4–7 and 9(C).

362 **Occurrence**: VPPLT 004, 264, 701, 706 and (partially) 1683 - MT 18 were collected in the
363 La Victoria Formation, upper Middle Miocene (Serravalian; see Figs. 3–6 for more details
364 on the stratigraphic provenance of individual specimens), while the UCMP 39846 and part
365 of VPPLT 1683 - MT18 comes from the Villavieja Formation, upper Middle Miocene
366 (Serravalian).

367 **Description**: For the original and detailed description of this species, including its
368 osteoderms, see Edmund and Theodor (1997). See the Tables 1 and 2 for an updated
369 compilation of osteoderm measurements of the *Scirrotherium* species and comparisons
370 with those of related taxa. Below there are descriptions of osteological structures and traits
371 incompletely known or unknown for *S. hondaensis* so far.

372 *Skull*: The holotype of *S. hondaensis* UCMP 40201 includes a very fragmentary
373 skull. This specimen does not preserve the anterior end of the rostrum, much of the orbit

(both dorsally and ventrally), part of the upper dental series, ear region, braincase and occipital region. In comparison, the skull VPPLT 706 (Fig. 4) described here, is more complete, despite the fact that it is also missing some structures. This new, small skull (see Table 3 for morphometric comparisons) is relatively well preserved from the orbit to the anterior end of rostrum, except for the anterior zygomatic arch and nasal bones. It also has a less deformed rostrum than the holotypic skull. The general aspect of the new skull is similar to those of other pampatheriids. In lateral view, it is markedly depressed towards its anterior end. In dorsal view, it is also tapered towards its anterior tip, where it ends abruptly (Castellanos, 1937). Proportionally, the rostrum is shorter than that of *K. paranensis* and even more than that of *H. floridanus*. In lateral view, the facial process of premaxilla is less well defined than that of *H. floridanus*, although the premaxilla-maxilla suture has a convex form like the latter species (Gaudin and Lyon, 2017). The antorbital fossa is arranged more vertically than those of *K. paranensis* and *H. floridanus*. The lacrimal is, proportionally, the largest among pampatheriids. This bone precludes the frontomaxillary contact (restricted contact in the skull of *K. paranensis*). The dorsal contribution of the lacrimal to the orbit is, proportionally, greater than in *H. floridanus* but similar to that in *K. paranensis*. The anterior root of zygomatic arch is projected posterolaterally, unlike other pampatheriids whose skull is known, where the anterior root projects laterally. The frontals show a conspicuous convexity in a position posterior to the insertion of the anterior root of zygomatic arch. In dorsal view, the frontals are more anteroposteriorly elongated and more laterally expanded than in *K. paranensis*, but are similar to those of *Holmesina* spp. In ventral view, the hard palate has a wide aspect, since the rostrum is shortened in comparison with other pampatheriids. Only two anterior molariforms are preserved (the left Mf1 and the right Mf2), so inferences about upper dentition are made from the alveoli. The

upper dental series, as in all the members of the family, is comprised of by nine molariforms. Of these, the last five (Mf5-Mf9) are bilobed. The anterior molariforms (Mf1-Mf4) converge anteriorly, but do not imbricate. The latter teeth are rounded to elliptical, similarly to the condition observed in *H. floridanus*. They also are less mesiodistally elongated than in *K. paranensis*. The molariforms with greatest occlusal area are the Mf5 and Mf6. The occlusal area of the upper molariforms decrease distally from the fifth and sixth molariforms to the ninth, as in all the pampatheriids. The Mf9 is the smallest of lobed molariforms and has the least degree of lobulation (elliptical shape for this tooth in the type material of *S. hondaensis*, according to Edmund and Theodor 1997). In ventral view, VPPLT 706 is characterized by a gradual transverse widening of the palatal portion of the maxilla from the level of the anterior border of the Mf5. The anterior portion of the palatines is preserved up to a level slightly posterior to the Mf9. The maxilla-palatine suture is not recognizable.

Femur: This bone in *S. hondaensis* was largely unknown so far, except for a pair of epiphyses (proximal and distal) from a left femur in the UCMP collections (UCMP 39846). VPPLT 706 preserves a left femur (Fig. 5(A–D)) without epiphyses (apparently it is not the same bone from which the previously noted epiphyses came). Thus, the description of all these anatomical elements allows for a reconstruction of most aspects of femoral anatomy. The estimated proximo-distal length of this bone is ca. 162 mm, and its transverse width at the third trochanter is 27.6 mm. These morphometric values are the smallest known for femora of Pampatheriidae (Table 4). They are comparable only to those of MLP 69-IX-8-13A which was referred to as *K.* cf. *paranensis* (Góis 2013; Scillato-Yané et al. 2013). The femoral head is hemispheric and the greater trochanter is less high than that of *K.* cf.

421 *paranensis*, but similar to the condition observed in *H. floridanus*. However, the greater
422 trochanter has a more tapered proximal end than in the latter species. In *S. hondaensis*, the
423 lesser trochanter is less mediolaterally expanded than in *K.* cf. *paranensis*. The femoral
424 diaphysis is less curved mediolaterally than in *K.* cf. *paranensis*, similar to that of *H.*
425 *floridanus*. The laterodistal border of the femur is more curved than in *H. floridanus*,
426 similar to that of *K.* cf. *paranensis*. The third trochanter is, proportionally, larger than that
427 of *K.* cf. *paranensis*, but is smaller than that of *H. floridanus*. The patellar facets are less
428 defined or delimited than those of *K.* cf. *paranensis*. In *S. hondaensis* these facets are
429 oriented toward the center of the anterior surface of the distal epiphysis, rather than
430 laterally as in *K.* cf. *paranensis* and *H. floridanus*.

431 *Ulna*: This bone is described here for the first time in *S. hondaensis*. A right ulna
432 (Fig. 5(E–H)) missing part of the diaphysis and the distal epyphysis is preserved in VPPLT
433 706. The estimated proximo-distal length is 89.5 mm. The olecranon is elongated and
434 protuberant. In medial view, it is less proximally tapered than that of *H. floridanus*. The
435 lateral entrance to the trochlear notch is very restricted, similarly to *Holmesina*. Likewise, it
436 is less proximo-distally elongated than that of *H. floridanus*. Proximally, at the level of the
437 trochlear notch, the posterior border is uniformly convex, not slightly concave as it is in *H.*
438 *floridanus*. The depression for the insertion of the anconeus muscle is deep and proximally
439 located, like that of *Holmesina*.

440 *Vertebrae*: Several vertebrae are also preserved in VPPLT 706 (Fig. 6). One of
441 these is a thoracic vertebra and five are caudal vertebrae, of which four are articulated in
442 two pairs and one is an isolated distal caudal vertebra. The body of the thoracic vertebra is
443 eroded anteriorly, as are the anterior zygapophyses. Posteriorly, the vertebral body has an

444 outline similar to that of other pampatheriids. Notably, two ventrolateral apophyses are
445 projected from the vertebral body. Although fragmented, the neural spine of the same
446 vertebra appears to be proportionally shorter than in *H. floridanus*. The anterior caudal
447 vertebrae have a posteriorly oriented and tall neural spine. The transverse processes are
448 relatively short.

449 *Astragalus*: Edmund and Theodor (1997) mentioned the existence of numerous
450 undetermined postcranial elements whose description was to be postponed to a subsequent
451 publication. However, that description was never published. This postcranial material from
452 the UCMP collections includes a left astragalus (UCMP 39846; Fig. 7(A–D)). In dorsal
453 view, the lateral trochlea is considerably larger than the medial trochlea. The astragalar
454 head is bulging, spherical, and almost uniformly convex. There is a shallow concavity in
455 the dorsal margin of the astragalar head whose function has been not determined, but it
456 could be for tendinous insertion. The astragalar neck is well-differentiated, similar to that in
457 *Holmesina*. In ventral view, the facets of articulation with the calcaneum, i.e., ectal and
458 sustentacular, are widely separated, as one would expect by observing their counterparts on
459 the calcaneum (Edmund 1987). The ectal facet is noticeably larger than the sustentacular
460 facet, in contrast to the condition in *H. floridanus*. The ectal facet is kidney-shaped and the
461 sustentacular facet has a sub-oval shape. Both of them are concave, especially the ectal
462 facet, which is very deep. The sustentacular facet is located in a central position within the
463 astragalar neck.

464 *Calcaneum*: This bone is other postcranial element not described by Edmund and
465 Theodor (1997) for *S. hondaensis*. UCMP 39846 is a well-preserved left calcaneum (Fig.
466 7(E–F)). It has proximo-distal length of 54.12 mm and a width at the level of facets (ectal

and sustentacular) of ca. 10.2 mm. These values are the smallest known for calcanei referred to as Pampatheriidae. The only species whose calcaneum is comparable in size to that of *S. hondaensis* is *H. floridanus*. The calcaneum of the latter species is slightly more proximo-distally elongated than in *S. hondaensis*, but it is roughly two times wider at the level of the ectal and sustentacular facets. This means that the calcaneum of *H. floridanus* is more robust than that of *S. hondaensis*. The calcaneal head is anteroposteriorly elongated, like in *H. floridanus* and unlike the proportionally short calcaneal head of *H. septentrionalis*. The anterior end of the calcaneal head is less shortened than that of *Holmesina*. The calcaneum of *S. hondaensis* shows no contact between the ectal and sustentacular facets, similar to the condition in species of *Holmesina* other than *H. floridanus* (Góis 2013). These facets are slightly convex and they are separated by a moderately deep and very wide groove, i.e., the sulcus tali (see below). Like *H. floridanus*, the facets are highly asymmetrical, but the condition in *S. hondaensis* is even more exaggerated, as the ectal facet is much larger than the sustentacular facet. As in the astragalus described above, the ectal facet is kidney-shaped and the sustentacular facet is sub-oval. The ectal facet is located at an oblique angle with respect to the long axis of the tuber calcanei, unlike that of *H. floridanus*. Like other pampatheriids, the calcaneal sustentacular facet of *S. hondaensis* is located anterior to the anterior border of the ectal facet. However, this facet is even more anteriorly placed in *S. hondaensis* than in other pampatheriid species as consequence of its particularly wide sulcus tali. Posteriorly, the calcaneal tuber is not massive in comparison with Pleistocene species of *Holmesina* (e.g., *H. septentrionalis*), but rather mediolaterally compressed, particularly towards its dorsal side.

Scirrotherium antelucanus Laurito and Valerio, 2013

LSID. urn:lsid:zoobank.org:act:225CD304-3B63-4B55-B8B8-33B46C90A194

Holotype. CFM-2867, mobile osteoderm (Laurito and Valerio, 2013).

Type locality and horizon. San Gerardo de Limoncito, County of Coto Brus, Province of Puntarenas, Costa Rica. Upper Curré Formation, Upper Miocene (Laurito and Valerio). For further information about the stratigraphic position of the Curré Formation, see these references: Lowery 1982; Yuan 1984; Rivier 1985; Kolarsky et al. 1995; Alvarado et al. 2009; Aguilar et al. 2010; Obando 2011. There are no published absolute ages for this geological unit.

Diagnosis. Unmodified (see Laurito and Valerio, 2013; p. 47).

Referred material. MUN STRI 36880, an isolated fixed osteoderm (Fig. 8).

Occurrence. Upper Sincelejo Formation, Upper Miocene to Pliocene (Messinian to Zanclean). El Coley Town, Municipality of Los Palmitos, Department of Sucre, Colombia. For further information about the stratigraphic position of the Sincelejo Formation, see these references: Flinch 2003; Villarroel and Clavijo 2005; Bermúdez et al. 2009; and Alfaro and Holz 2014. There are no published absolute ages for this geological unit.

Remarks. The fixed osteoderm MUN STRI 36880, possibly from the of the pelvic shield, is assigned to the species *S. antelucanus* on the basis of the following observations: (I) the area and thickness of this osteoderm (linear measurements in millimetres: anteroposterior length = 34.91; transverse width = 24; thickness = 4.45; approximate area = 837.8 mm^2) are

within the range of variability for comparable osteoderms of *S. antelucanus* and exceed the known values of area for most of the same kind of osteoderms for *S. hondaensis*; (II) the external surface is relatively smooth; (III) the anterior margin is wide; (IV) the anterior foramina are larger (2–3 millimetres of diameter) than in *S. hondaensis*, like *S. antelucanus* from Costa Rica; (V) the number of anterior foramina (9) is within the range of variability for *S. antelucanus* (7–10 for quadrangular osteoderms, like the specimen here described), but greater than the range for *S. hondaensis*; (VI) poorly elevated longitudinal central elevation, like in some osteoderms of *S. antelucanus* (the longitudinal central elevation is generally more elevated in *S. hondaensis*; see Laurito and Valerio 2013).

aff. *Scirrotherium*

Referred material: MUN STRI 16718 (Fig. 9(A)), fixed osteoderm of the scapular shield; MUN STRI 38064 (Fig. 9(E)), undetermined fixed osteoderm; MUN STRI 16719 (Fig. 9(G)), mobile osteoderm fragmented in its anterior margin.

Occurrence: Castilletes Formation, upper Lower Miocene to lower Middle Miocene, upper Burdigalian to Langhian). Localities of Makaraipao, Kaitamana and Patajau Valley (localities with numbers 390093, 430202 and 390094 in Moreno et al. 2015, respectively), Municipality of Uribia, Department of La Guajira, Colombia.

Description: The fixed osteoderm of the scapular shield MUN STRI 16718 (Fig. 9(A)) is relatively large and has a pentagonal outline. Its linear measurements in millimetres are: anteroposterior length = 45.02; transverse width = 33.41; thickness = 6.66. These values imply that this osteoderm has greater area than any other known area size for osteoderms

533 referred to as *Scirrotherium* (Table 1), including those of the osteoderms of the larger
534 *Scirrotherium* species, i.e., *S. antelucanus* (see Appendix 1 in Laurito and Valerio 2013).
535 Rather, this osteoderm is similar in size to those reported for *H. floridanus*. The external
536 surface of the osteoderm MUN STRI 16718 is punctuated by numerous diminutive pits,
537 like *S. hondaensis* and *S. antelucanus*. The surface does not have a recognizable
538 longitudinal central elevation nor longitudinal depressions, so that the osteoderm has a
539 flattened appearance, similar to that of several osteoderms of *S. antelucanus* (Laurito and
540 Valerio 2013). In contrast, the marginal elevations are easily identifiable. These ridges are
541 relatively low and narrow. There are foramina with a nearly homogeneous large size in the
542 anterior margin. They are aligned in two well defined rows. The most anterior row has five
543 foramina and the posterior one has six. Collectively, the two rows of foramina rows are
544 equivalent to ca. 25% of the anteroposterior length of the osteoderm. In *S. hondaensis*, the
545 rows of foramina in fixed osteoderm, when present, this percentage comprises less than
546 20%.

547 The osteoderm MUN STRI 38064 (Fig. 9(E)) does not appears to be a non-marginal
548 osteoderm. It has a trapezoidal outline and the following measurements in millimetres:
549 anteroposterior length = 39.08; transverse width = 39.55; thickness: 5.98. These values are
550 within the range of variability of *S. antelucanus*. This osteoderm has two long rows of
551 anterior foramina in which the posterior row seems to extend partially over the anterior
552 lateral margins, unlike the anterior foramina row(s) in *S. hondaensis* and *S. antelucanus*.
553 The most anterior row of foramina is formed by eight foramina and the posterior row has
554 11 foramina. In both of these rows, the foramina are of similar size, although a few are
555 smaller. The rows of foramina diverge on the left lateral margin and within the resultant

556 space between these rows is located a large and isolated foramen. This osteoderm does not
557 have a recognizable longitudinal central elevation nor longitudinal depressions, i.e., it is
558 flattened. Its marginal elevations are narrow and poorly elevated. The foramina of the
559 lateral margins are smaller than most of anterior foramina. As a consequence of
560 preservation factors, the pits on the external surface are not present.

561 The osteoderm MUN STRI 16720 is a partial mobile osteoderm (Fig. 9(G)) with an
562 elongated rectangular shape. Its linear measurements in millimetres are: anteroposterior
563 length (incomplete by fragmentation) = 45.68; transverse width = 30.69; thickness = 6.96.
564 The external surface is convex and without a longitudinal central elevation or longitudinal
565 depressions. The anterior margin shows a set of foramina not clearly aligned in rows.

566 **Remarks**: With current evidence, the osteoderms MUN STRI 16718 and MUN STRI
567 38064 could not be confidently assigned to *Scirrotherium*. This taxonomic decision is
568 supported by several arguments. First, morphologically, the osteoderms referred here to aff.
569 *Scirrotherium* are more similar to those of *S. hondaensis* and *S. antelucanus* than to any
570 other osteoderms of known pampatheriids. The osteoderms of aff. *Scirrotherium* differ with
571 respect to the osteoderms of *S. hondaensis* and *S. antelucanus* in three characteristics: (I) a
572 greater number of anterior foramina and/or greater development of two rows from these
573 foramina; (II) longitudinal central elevation possibly absent, i.e., the presence of a flattened
574 external surface; (III) larger maximum osteoderm area. Of these features, the third one (III)
575 is the least ambiguous, i.e., the maximum area of fixed osteoderms exceeds those of the
576 osteoderms of *S. hondaensis* and *S. antelucanus*. Comparatively, the first and second (I and
577 II) characteristics are more ambiguous considering that similar conditions were also
578 observed in *S. hondaensis* and *S. antelucanus*. These conditions are described as follows.

579 Some infrequent osteoderms of *S. hondaensis* have two anterior rows of foramina, of which
580 the anterior row is comparatively less developed (i.e., with smaller and fewer foramina)
581 than in aff. *Scirrotherium*. Additionally, in *S. hondaensis* and, particularly in *S.*
582 *antelucanus*, some osteoderms have a flattened or even a missing longitudinal central
583 elevation. These observations imply limitations on the taxonomic resolution, especially
584 considering that the material on which aff. *Scirrotherium* is based is scarce and does not
585 allow comparisons of a representative series of osteoderms encapsulating the
586 morphological variability within the carapace of this animal.

587

588 ***Kraglievichia*** Castellanos, 1927

589 *LSDI.* urn:lsid:zoobank.org:act:92C8B169-4F79-467E-B951-EF1DE6E327B1

590 **Type species**: *Kraglievichia paranensis* Ameghino, 1883

591 **Other referred species**: *Kraglievichia carinatum* comb. nov. (= *Scirrotherium carinatum*
592 Góis, Scillato-Yané, Carlini and Guilherme, 2013; see below)

593 **Emended differential diagnosis**: Small-to-middle sized pampatheriid characterized by
594 fixed osteoderms with ornamentation (particularly the longitudinal central elevation) more
595 conspicuous than in any other pampatheriid; anteriorly wide and posteriorly tapered
596 longitudinal central elevation; very deep longitudinal depressions; highly elevated and
597 frequently blunt marginal elevations, even flattened towards their top; external surface of
598 osteoderms generally rougher than in *Scirrotherium* but less than in *Holmesina*.

599

Kraglievichia carinatum comb. nov.

2013. *Scirrotherium carinatum* – Góis, Scillato-Yané, Carlini and Guilherme, Fig. 4.

Holotype: MLP 69-IX-8-13-AB, a mobile osteoderm (Góis et al. 2013).

Type locality and horizon: Paraná River cliffs, Province of Entre Ríos, Argentina. Ituzaingó Formation, Upper Miocene, Tortonian (Góis et al. 2013).

Differential diagnosis: Unmodified (see Góis et al. 2013, p. 182).

Referred material: The holotype, paratypes and part of the hypodigm of this species (see Fig. 10 and Appendix S1 of the Supplementary Material).

Discussion. In their descriptive work on *K. carinatum* comb. nov., Góis et al. (2013) did not explicitly justify the inclusion of this species within *Scirrotherium*. Interestingly, part of the material assigned to the taxon they create, coming from northwestern Brazil (Solimões Formation), was previously referred to as *Kraglievichia* sp. by several researchers, including Góis himself (Góis et al. 2004; Góis 2005; Cozzuol 2006; Latrubesse et al. 2010; Góis et al. 2013). However, Góis et al. (2013) refuted the original taxonomic assignment, arguing that it was erroneous, although they did not offer any concrete support for their decision. In the absence of a phylogenetic analysis in Góis et al. (2013), we could assume by default that these authors included *K. carinatum* comb. nov. within *Scirrotherium* because they considered osteoderm features of this species at least compatible with the generic diagnosis proposed by Edmund and Theodor (1997). Based on morphological similarity, Góis and colleagues hypothesized closer affinities between *K. carinatum* comb. nov. and *S. hondaensis* than those between *K. carinatum* comb. nov. and *K. paranensis*.

First, it is necessary to analyse in detail each of the osteoderm features of *K. carinatum* comb. nov. in relation to the original diagnosis of *Scirrotherium*. According to Edmund and Theodor (1997), the fixed osteoderms of *Scirrotherium* have a small (not specified) number of large piliferous foramina on the anterior margin. These foramina are well spaced but interconnected by a distinct channel. This is observed both in *K. carinatum* comb. nov. and *S. hondaensis*. Likewise, the presence of continuous marginal elevations, posteriorly confluent with the longitudinal central elevation, is a trait also shared by the two compared species. Finally, the relative osteoderm size of *K. carinatum* comb. nov. is small relative to other pampatheriids, which is in line with the original diagnosis for *Scirrotherium*.

Therefore, the osteoderm features of *K. carinatum* comb. nov. are compatible with those mentioned in the diagnosis for *Scirrotherium* by Edmund and Theodor (1997). However, this does not necessarily imply that the taxonomic allocation of *K. carinatum* comb. nov. to the genus *Scirrotherium* is correct. In fact, there are several reasons to consider this assignment is unreliable. Initially, the diagnosis of Edmund and Theodor (1997) contained only three allegedly diagnostic osteoderm features, including the relative osteoderm size. Furthermore, and more importantly, these "diagnostic features" do not allow definitive discrimination between *Scirrotherium* and any other genus of pampatheriids. Indeed, in their analysis, Góis et al. (2013) accept that, for instance, *Vassallia minuta* also shares the presence of fixed osteoderms with a small number of large anterior foramina, which are well spaced and connected by a canal. Independently, Laurito and Valerio (2013) also highlighted the non-diagnostic nature for *Scirrotherium* of the latter osteoderm trait. The other osteoderm features under consideration, i.e., the posterior confluence of the marginal elevations with the longitudinal central elevation and the small osteoderm size, are also of

644 ambiguous diagnostic value. For instance, the confluence of marginal elevations and
645 longitudinal central elevation is also found in *K. paranensis*, a pampatheriid clearly
646 different from *Scirrotherium*. And although apparently informative on body-size trends of
647 some individual pampatheriid lineages (e.g., *Holmesina* spp.) and useful as discriminant
648 factor between species (Góis et al. 2013; Laurito and Valerio 2013), the relative osteoderm
649 size is not necessarily sufficient to make taxonomic assignments to the genus level among
650 pampatheriids as a whole (see below). In this sense, it is worth noting the potentially
651 conflicting taxonomic conclusions that could be reached using osteoderm-inferred relative
652 body size versus those based on non-osteoderm evidence. For example, MLP 69-IX-8-13A,
653 a femur belonging to an adult individual from the Ituzaingó Formation, was assigned to *K.*
654 cf. *paranensis* by Scillato-Yané et al. (2013), is comparable in size to that of the small
655 pampatheriid *S. hondaensis*. Therefore, it is probable that the referred femur does not
656 belong to the medium-to-large sized *K. paranensis*, although it is reasonable to include it in
657 the genus *Kraglievichia* (as the authors decided). However, Scillato-Yané et al. (2013) did
658 not discuss the possibility that the material assigned to *K.* cf. *paranensis*, particularly MLP
659 69-IX-8-13A, might be related to the (partially) co-occurrent species of *K. paranensis*, i.e.,
660 *K. carinatum* comb. nov., a pampatheriid whose small body size is fully compatible with
661 the small size of that femur. In other words, like Góis et al. (2013), they did not seriously
662 consider the hypothesis of *K. carinatum* comb. nov. as a small species of *Kraglievichia*,
663 rather than a species belonging to *Scirrotherium*.

664 Again analysing the original diagnosis of *Scirrotherium* by Edmund and Theodor (1997), it
665 should be regarded as ambiguous and hardly useful to differentiate this genus from other
666 genera in Pampatheriidae, at least with respect to osteoderm traits. It is likely that these

667 supposedly diagnostic features are actually symplesiomorphies for the entire family or, at
668 most, a hypothetical subfamilial lineage. This means that Góis et al. (2013) did not have a
669 sufficiently robust diagnosis of *Scirrotherium* to confidently assign *K. carinatum* comb.
670 nov. to this genus. Alternatively, they may have noted morphological similarity between
671 osteoderms of *K. carinatum* comb. nov. and *S. hondaensis* from features not included in the
672 diagnosis by Edmund and Theodor (1997). However, Góis et al. (2013) only listed
673 morphological differences between these species and virtually did not mention any
674 similarity for them, except for potentially equivocal resemblance as that indicated by
675 relative osteoderm size (i.e., small osteoderm sizes in comparison with those of *K.*
676 *paranensis* and *Plaina*). The lack of usefulness of the relative osteoderm size for generic
677 assignation is further supported by the osteoderm morphometric analysis in Góis et al.
678 (2013, p. 185), whose resulting PCA and CCA plots show that, despite the similarity in
679 relative osteoderm size, *K. carinatum* comb. nov. is located far from *S. hondaensis* (which
680 is closer to *V. minuta*, a taxon apparently related to other main lineage within
681 Pampatheriidae, i.e., *Plaina-Pampatherium*) and *K. paranensis* in morphospace.

682 Summarizing, there is little justification by Góis et al. (2013) on their taxonomic decision
683 to including *K. carinatum* comb. nov. within *Scirrotherium*. Considering the morphological
684 conservatism of Pampatheriidae, the observation of a common general morphological
685 pattern between *K. carinatum* comb. nov. and *S. hondaensis* does not necessarily imply the
686 grouping of these species under the same generic taxon, least of all by omitting the
687 taxonomic significance of striking similarities in osteoderm ornamentation between *K.*
688 *carinatum* comb. nov. and the better known taxon *K. paranensis*. Furthermore, we should
689 note that Góis and colleagues, in their work on *K. carinatum* comb. nov., did not make

morphological comparisons including to *S. antelucanus*, a species more similar in osteoderm features to *S. hondaensis* (i.e., the type species of *Scirrotherium*). The species *S. antelucanus* was described on a scientific article (Laurito and Valerio 2013) published nearly simultaneously, but later, to that of *K. carinatum* comb. nov. Therefore, Góis et al. (2013) did not know about the existence of *S. antelucanus* when they performed their systematic analysis ("Until the present study, *S. hondaensis* was the only known species of this genus"; Góis et al. 2013, p. 177), so that their taxonomic assignment of *K. carinatum* comb. nov. to *Scirrotherium* was likely the result of limited notions on the morphological variability and diversity of *Scirrotherium* in northern South America and southern Central America.

In this work I decide to assign *K. carinatum* comb. nov. to the genus *Kraglievichia* based on the results of phylogenetic analyses that I designed considering the hypothesis of Edmund (1985) on the probable subfamilial relationships within Pampatheriidae, which implicitly sustains that the creation of supraspecific taxa from osteoderm evidence should be determined –with the prerequisite of morphological similarity- by the degree of development of the ornamentation. Understanding that *K. carinatum* comb. nov. has morphologically similar osteoderms to those of *K. paranensis* (apart from relative osteoderm size) and has one of the more conspicuous, protuberant osteoderm ornamentations among pampatheriids, along with *K. paranensis*, as acknowledged by Góis et al. (2013) themselves, this means that *K. carinatum* comb. should be considered closely related to *K. paranensis* and therefore they both should also be included in the same genus, i.e., *Kraglievichia*.

5. Discussion

5.1. Systematic implications

This systematic analysis is the first attempt to test the intergeneric relationships and internal structure of the genus *Scirrotherium* with its three previously referred species, i.e., *S. hondaensis* (type species), '*S.*' *carinatum* (= *K. carinatum* comb. nov.) and *S. antelucanus*. The two strict consensus trees from the distinct character weighting schemes (equal and implied weights) show very similar results. However, the preferred phylogenetic hypothesis is that supported by the implied weights analysis. According to Goloboff et al. (2018), the parsimony analysis under implied weights outperforms equal weighting and the model-based methods. Beyond this preference for a particular hypothesis (further supported below), both resultant trees agree that the species referred to as *Scirrotherium* are not monophyletic and, consistently, from a diagnostic point of view only *S. hondaensis* and *S. antelucanus* appears as those actually referable to *Scirrotherium*. The relationship between *S. hondaensis* and *S. antelucanus* could not be confidently resolved, despite the inclusion of new osteoderm characters (the only ones comparable between these species so far) in these parsimony analyses. Consequently, a paraphyletic relationship among *S. hondaensis* and *S. antelucanus* should not be rule out. In conjunction, these results suggest the need of information on craniomandibular or dental characters for *S. antelucanus* to further test the affinities of this species with respect to *S. hondaensis*. Until new phylogenetic evidence is available, *Scirrotherium* is maintained as taxonomically valid using a new, emended diagnosis which focus (in addition to specific osteoderm similarities between *S. hondaensis* and *S. antelucanus*) on its lesser degree of development of the osteoderm ornamentation in comparison with those in *Holmesina* and, particularly, *Kraglievichia*, but greater degree of

development than in the *Plaina-Pampatherium* lineage. This new diagnosis replaces the original and now inadequate diagnosis by Edmund and Theodor (1997).

Unlike the unpublished phylogeny of Góis (2013), the phylogenetic position of '*S.*' *carinatum* was resolved here, i.e., this species is the sister taxon of *K. paranensis*. Therefore, it is proposed the new name *K. carinatum* comb. nov. Despite Góis (2013) did not recover as a clade to *S. hondaensis* and *K. carinatum* comb. nov., as expected if both these species were assigned to *Scirrotherium*, he presented one supposed synapomorphy that join them, i.e., very deep longitudinal depressions, "in particular in *S. carinatum*" (Góis 2013, p. 215). This feature is not a confident support for grouping *S. hondaensis* and *K. carinatum* comb. nov. because the deepest longitudinal depressions in this pampatheriid lineage are found in *K. carinatum* comb. nov. and *K. paranensis*, not in *S. hondaensis*. The new emended differential diagnosis for *Kraglievichia* acknowledges the highly sculpted external osteoderm surface documented on this taxon, which is more protuberant than in the Plio-Pleistocene genus *Holmesina*. This diagnosis provides an updated and concise description of useful osteoderm features to distinguish *Kraglievichia* from other genera within Pampatheriidae. It is important to note that the species *K. paranensis* has several autapomorphies (see Appendix S4 of the Supplementary Material) which, in addition to the relative osteoderm size, need to be compared in the future with homologous, unknown endoskeletal traits in *K. carinatum* comb. nov. in order to test the phylogenetic affinity of these two species as inferred from osteoderm traits. Provisionally, the difference in relative osteoderm size (consequently also in relative body size) and some morphological differences between *K. carinatum* comb. nov. and *K. paranensis*, as noted by Góis et al. (2013), may be linked to distinct ontogenetic growth trajectories in these species, with *K.*

759 *carinatum* comb. nov. representing the plesiomorphic condition (i.e., small body size; see
760 Sánchez-Villagra 2012 for a discussion on the implications for taxonomy of the ontogenetic
761 growth in extinct species).

762 Other important difference here with respect to the phylogeny of Góis (2013) is that *K.*
763 *paranensis* was not recovered as the one single sister taxon of *Holmesina* spp. (except *H.*
764 *floridanus*). Instead, it is part of a group additionally formed by *S. hondaensis*, *S.*
765 *antelucanus* and *K. carinatum* comb. nov. Together, these taxa are the sister clade of
766 *Holmesina*. This means that we do not have evidence of direct ancestral forms to
767 *Holmesina* yet. However, despite some striking differences, it is remarkable the greater
768 morphological similarity of the osteoderm ornamentation and several cranial features
769 between *Holmesina* (especially *H. floridanus*) and *Scirrotherium*, rather than with those of
770 *Kraglievichia*. The recognizable similarities between *H. floridanus* and *S. hondaensis*, and
771 at the same time differences with *K. paranensis*, include less protuberant osteoderm
772 ornamentation; occurrence of uniformly narrow longitudinal central elevation in fixed
773 osteoderms; more robust skull; more expanded frontals; the plane of the frontals forming a
774 reflex angle with that of the parietals; less anteroposteriorly elongated upper teeth; and the
775 first two upper molariforms less obliquely oriented with respect to the midline of the hard
776 palate.

777 Góis (2013) found that *Holmesina* is non-monophyletic due to the phylogenetic position of
778 *H. floridanus* with respect to the other *Holmesina* species. This result coincides with that
779 recovered here from the parsimony analysis with equal weights. *Holmesina floridanus* has
780 several plesiomorphic features in comparison with the remaining *Holmesina* species, e.g.,
781 less protuberant ornamentation, less rough external surface of the osteoderms and less

782 dorsally situated basicranium with respect the palatal plane. However, the confluent
783 arrangement of the calcaneal facets of the astragalus in *H. floridanus* suggests that this
784 species might not be directly related to any known South American pampatheriid (Edmund
785 1987). Likewise, Gaudin and Lyon (2017) have recently found potential support for the
786 monophyly of *Holmesina* from craniomandibular specimens. Therefore, the position of *H.*
787 *floridanus* in a polytomy with *S. hondaensis* and *S. antelucanus* in the analysis with equal
788 weights is explained from the lack of resolution (relatively small character sampling by a
789 fragmentary fossil record and homoplastic noise), not as product of a "real" non-
790 monophyletic relationship with the remaining *Holmesina* species. Conversely, the
791 *Holmesina* is recovered as monophyletic by the implied weights analysis. As expected, in
792 this topology *H. floridanus* is the most basal species of *Holmesina*. In both strict consensus
793 trees, *H. septentrionalis*, the other North American species, is grouped together with all the
794 South American *Holmesina* species (except *H. rondoniensis* and *H. cryptae*, both excluded
795 in this study).

796 I abstained from revising the diagnosis of *Holmesina* because this is considered beyond the
797 intended objectives of this work. However, six putative synapomorphies (unambiguous and
798 ambiguous) are proposed (or further supported) for this genus: (1) Anterior and lateral
799 margins with elongated, strong bone projections as radii directed from the external border
800 of the central figure towards the osteoderm borders in non-marginal fixed osteoderms; (2)
801 anteriorly convergent, nearly in contact medial processes of premaxillae; (3) length of
802 nasals greater than 30% of the maximum anteroposterior length of the skull; (4)
803 conspicuous and anteroposteriorly elongated maxillary ridge (Gaudin and Lyon 2017); (5)

804 relatively small lacrimal; and (6) bilobed posterior upper molariforms (Mf5-Mf9) with
805 incipient trilobulation.

806

807 *5.2. Evolutionary and biogeographic implications*

808 *Scirrotherium* is a pampatheriid genus from the Early Miocene-Late Pliocene of northern
809 South America and southern Central America. This taxon, along with *Kraglievichia*, forms
810 the sister group of *Holmesina* (Fig. 11), a pampatheriid probably originated in tropical
811 southern North America (Mexico? see Woodburne 2010). However, based on the
812 osteological comparisons presented above, which are expanded with respect to those of
813 Edmund (1987), the hypothetical South American ancestor or sister taxon of *Holmesina*
814 probably was morphologically generalized, more similar to *Scirrotherium* or aff.
815 *Scirrotherium* than to *Kraglievichia*. This interpretation is in line with that of Edmund
816 (1987), according to which the calcaneo-astragalar articulation of *S. hondaensis* challenges
817 the hypothesis that this pampatheriid is ancestral to *H. floridanus*, but the ornamentation
818 pattern of the osteoderms suggests "at least some degree of relationship" with the latter
819 species. Anatomically, *Kraglievichia* should be considered a highly divergent taxon,
820 especially to taking into account its Miocene age. According to Edmund (1987, p. 16), "the
821 osteoderms [of *H. floridanus*] are quite dissimilar to those of *Kraglievichia*". This
822 interpretation is shared in this work and contrasts with that of Scillato-Yané et al. (2005),
823 which suggested that *Holmesina* originated from a hypothetical South American basal form
824 of *Holmesina* or *Kraglievichia*. It also is opposed to Simpson (1930) and to the phylogeny
825 of Góis (2013) in which *Kraglievichia* is the only sister taxon of *Holmesina*.

826 The earliest record of *Scirrotherium*, here treated as tentative by scarce and poorly
827 preserved material, comes from the Early Miocene (late Burdigalian) of northwestern
828 Venezuela (Rincón et al. 2014; see below). Independently from the validity of occurrence
829 of *Scirrotherium* in an Early Miocene locality of northern South America, this record
830 represents the oldest pampatheriid reported in the scientific literature so far. This
831 improvement makes the fossil record of Pampatheriidae more congruent with the expected
832 time of origination of this family, i.e., Late Oligocene-Early Miocene, according to the very
833 few available time-calibrated phylogenies including representatives of Pampatheriidae and
834 its sister group, Glyptodontidae (e.g., Fernícola 2008; Billet et al. 2011). Apparently, the
835 Early Miocene Venezuelan pampatheriid indicates an origin of these xenartrans in low
836 latitudes in South America. However, this hypothesis could be defied by a possible Late
837 Eocene pampatheriid of Argentina, which has been not formally described and published
838 yet (Góis 2013).

839 Beyond the geographic origin of Pampatheriidae, northern South America seems to have
840 been a critical area for the early diversification of, at least, the lineage including
841 *Scirrotherium*. This genus probably differentiated at least as early as the late Early
842 Miocene-early Middle Miocene (late Burdigalian-Langhian) in northernmost South
843 America. The former evolutionary inference is consistent with the late Early Miocene
844 record referred to as *Scirrotherium* from Venezuela (Rincón et al. 2014).

845 Collectively, *Scirrotherium* and *Kraglievichia* occupied a large area in South America
846 during the Neogene (Fig. 12). The geographic range of *Scirrotherium* was more restricted
847 than that of *Kraglievichia*, comprising only tropical low latitudes, instead of a wide
848 latitudinal range, as suggested by Góis et al. (2013). The revaluated distributional pattern of

849 *Scirrotherium* is comparable to that of the glyptodontid *Boreostemma*, which is recorded
850 from the Middle Miocene to the Late Pliocene of Colombia and Venezuela (Carlini et al.
851 2008; Zurita et al. 2016). In contrast, the distributional range of *Kraglievichia* is similar to
852 that of other Miocene xenarthran taxa at the generic and specific level, which occurred in
853 southern South America and northwestern Brazil, but not in the northern or northwestern
854 end of South America (see Ribeiro et al. 2014).

855 Overall, this evidence indicating biogeographic divergence of northwesternmost South
856 America as an independent faunal province from the late Early Miocene to Middle
857 Miocene, and possibly into the Late Miocene or even the Early Pliocene, is consistent with
858 the results of multiple analyses of the South American terrestrial mammal fossil record for
859 the Neogene (Patterson and Pascual 1968; Cozzuol 2006; Ortiz-Jaureguizar and Cladera
860 2006; Croft 2007; Carrillo et al. 2015; Rincón et al. 2016; Kerber et al. 2017; Brandoni et
861 al. 2019). Apparently, the existence of one or several strong geographic and/or ecoclimatic
862 barriers (e.g., the Pebas Mega-Wetland System, whose expansion climax coincides with the
863 Middle Miocene) in northern South America would explain that regional endemism pattern
864 (MacFadden 2006; Croft 2007; Salas-Gismondi et al. 2015; Jaramillo et al. 2017). At the
865 same time, the development of a late Early-to-Middle Miocene biogeographic divergence
866 between northwesternmost South America and the rest of this continent may account for
867 the evolutionary divergence of *Scirrotherium* and *Kraglievichia*.

868 In the Late Miocene, without a completely formed Panamanian Land Bridge (O'dea et al.
869 2016), *Scirrotherium* expanded its geographic range to southern Central America (Fig. 12),
870 suggesting a possible ephemeral land connection or, more likely, overwater dispersal
871 between South America and Central America (maybe via rafting mechanism; efficient

872 active swimming of pampatheriids in a marine channel seems highly improbable). This is
873 the earliest dispersal event of a pampatheriid to North America (see below). The Central
874 American species of *Scirrotherium*, *S. antelucanus*, is larger than *S. hondaensis*, but
875 comparable or even smaller than aff. *Scirrotherium*. From available evidence, it is not
876 possible to determinate the most probable area of evolutionary differentiation of *S.*
877 *antelucanus*, but now there is support for occurrence of this species in the late Neogene of
878 northwestern South America, specifically in the Department of Sucre, Colombia.

879 The South American record of *S. antelucanus* is probably several million years younger (3–
880 5 my) than the Central American record. However, given the lack of absolute dating for the
881 fossil-bearing stratigraphic levels and the occurrence of Late Miocene strata in the same
882 geological unit (Sincelejo Formation) where comes the material here assigned to *S.*
883 *antelucanus* in Colombia, it should be recognized a significant age uncertainty for the new
884 South American record of this species. In any case, this age is considered may be Early
885 Pliocene or, alternatively, Latest Miocene from the stratigraphic position of the fossil-
886 bearing horizons (Villarroel and Clavijo, 2005; Bermúdez et al. 2009; Alfaro and Holz
887 2014; Bernal-Olaya et al. 2015; Córtes et al. 2018), as well as from associated
888 palynomorphs (Silva et al. 2012; B. Fernandes and C. Jaramillo, pers. comm. 2014).

889 The biogeographic correlation across the Isthmus of Panama using *S. antelucanus* has
890 insightful implications for the understanding of the late Cenozoic intercontinental migratory
891 dynamics in the Americas, including the Great American Biotic Interchange (GABI) (Webb
892 2006; Woodburne et al. 2006; Woodburne 2010; Cione et al. 2015; Bloch et al. 2016).
893 Noteworthy, this is the first transisthmian biogeographic correlation for a Neogene
894 terrestrial mammal at the level of species; furthermore, it is the first short-distance

intercontinental correlation (i.e., adjacent to the Central American Seaway) with high taxonomic resolution for Neogene land mammals of the Americas; and, finally, it constitutes the first evidence of a distributional pattern congruent with a re-entry event to South America by a pre-Pleistocene xenarthran.

We know a few biogeographic correlations across the Isthmus of Panama which are based on records at generic level of Neogene and Pleistocene land mammals, as well as a very few records at species level of the latter epoch. The Neogene biogeographic correlations include the pampatheriid genera *Plaina*, in Mexico and central-southwestern South America; *Pampatherium*, in Mexico and southeastern South America; and *Holmesina*, in the United States, Mexico and El Salvador, as well as in northwestern and southeastern South America (Woodburne 2010). At the level of species, for instance, the Pleistocene megatheriine *Eremotherium laurillardi* has occurrence in both sides of the Isthmus of Panama in North- and South America (Cartelle and De Iuliis 1995, 2006; Tito 2008; McDonald and Lundelius, E. L. Jr. 2009; Martinelli et al. 2012; Cartelle et al. 2015).

The record in South America of *S. antelucanus* increase the taxonomic resolution of transisthmian biogeographic correlations of Neogene land mammals, opening the possibility of new correlations of this kind and their biostratigraphic application in circum-Caribbean basins, in a similar way as envisioned by the renowned American palaeontologist Ruben A. Stirton from his revision of the fossil mammal remains of "La Peñata fauna" (Stirton 1953), the vertebrate fossil association where comes the new record of *S. antelucanus*. This translates into direct correlation of Land Mammal Ages (in this case, SALMA and NALMA) from migrant mammals which are shared at species level by both South and North America. Using to *S. antelucanus*, this would mean exists a support

for faunal, not necessarily chronological, correlation of the early Hemphillian and Montehermosan mammal (xenarthran) assemblages in North America and South America, respectively (see Laurito and Valerio, 2013). Naturally, any compelling intercontinental faunal correlation requires more than one taxonomic element for support. The direct intercontinental faunal correlations from Cenozoic land mammals between South and North America are still underdeveloped in comparison with those between other continents (e.g., North America and Europe or North America and Asia; Woodburne and Swisher, C. C. III 1995; Beard and Dawson 1999; Bowen et al. 2002)

Additionally, the transisthmian correlation of *S. antelucanus* allows to increase the geographic resolution in the detection of intercontinental migrations of late Cenozoic land mammals, which are restricted mainly to large and middle distance correlations for the Neogene record (e.g., Mexico-southern South America; Woodburne 2010). This pattern has prevented the exploration of possible early or intermediate phases of anagenetic/cladogenetic events in late Cenozoic Interamerican migrant taxa, which in turn it is reflected in the fact that we are detecting "suddenly" well-differentiated terminal taxa (e.g., *Holmesina*) in marginal, distant areas with respect to the Central American Seaway and adjacent terrains (Cione et al. 2015 and references therein).

On the other hand, the new transisthmian correlation here presented suggests a possible Neogene re-entry event by a xenartran to South America after its evolutionary differentiation in North America (Fig. 12). The confirmation of this depends on a confident determination of the differentiation area for *S. antelucanus*, i.e., if this species originated in South America, the new record is explained more parsimoniously by population maintenance in the ancestral area. Conversely, if this species originated in Central America

941 from a South American species of *Scirrotherium* as *S. hondaensis*, then we are considering
942 a re-entry event to South America. However, as mentioned above, it is not possible to
943 constrain much more than that at this moment. In any case, the possibility of a Neogene re-
944 entry event to South America by a xenarthran is compatible with the fact that we know
945 several of these events during the Pleistocene. Among these Pleistocene events, there are
946 several involved xenarthrans, including the pampatheriids *Holmesina* and *Pampatherium*,
947 the glyptodontid *Glyptotherium*, the pachyarmatheriid *Pachyarmatherium*, the dasypodid
948 *Dasypus* and the megatheriine *Eremotherium* (Woodburne et al. 2006; Woodburne 2010
949 and references therein).

950 On another note, the results of this work have evolutionary implications for the genus
951 *Holmesina* and the multiple Interamerican dispersal events of pampatheriids, including that
952 of *Scirrotherium* (discounting the non-confirmed re-entry event to South America). The
953 genus *Holmesina* has its oldest record (*Holmesina* sp.) in sedimentary rocks deposited
954 around the Pliocene-Pleistocene boundary (ca. 2.4 mya) in Florida, United States (Edmund
955 1987; Woodburne 2010 and references therein; Gaudin and Lyon 2017). This northward
956 dispersal event is part of the earliest phase of the GABI (GABI 1), in which additionally
957 participated other xenartrans as *Dasypus*, *Pachyarmatherium* and *Eremotherium*
958 (Woodburne 2010). Typically, *H. floridanus* has been considered the most basal among the
959 *Holmesina* species (Edmund 1987), as it is supported here. The hypothetical time-calibrated
960 phylogeny introduced in this work for Pampatheriidae (Fig. 11) suggests that exist a long
961 ghost lineage leading to *Holmesina*, from the Early Miocene (Burdigalian) until the Late
962 Pliocene. The improvement of the fossil record in northern South America, Central

963 America and Mexico will allow to advance in the recognition of probable direct ancestral
964 forms for *Holmesina*.

965 From the above analysis, a probable model of biogeographic evolution of *Holmesina* is as
966 follows (Fig. 12). A hypothetical pampatheriid close to *Holmesina* or even a hypothetical
967 *Holmesina* species basal with respect to *H. floridanus* dispersed to Central America,
968 Mexico and United States during the Pliocene (Early Pliocene according the time-calibrated
969 phylogeny). Once it was established the genus *Holmesina* in North America with *H.*
970 *floridanus*, the larger species *H. septentrionalis* diverged and differentiated in the Early
971 Pleistocene of southern United States. Later, *H. septentrionalis* expanded southward to
972 Mexico and Central America during the Early-Middle Pleistocene (Aguilar and Laurito
973 2009). In the Middle or early Late Pleistocene, possibly *H. septentrionalis* colonized South
974 America, where took place an important diversification, which was likely influenced by the
975 Late Pleistocene climatic changes (Scillato-Yané et al. 2005). This diversification gave
976 origin to the species *H. occidentalis*, *H. rondoniensis*, *H. cryptae*, *H. major* and the most
977 robust pampatheriid, *H. paulacoutoi* (Scillato-Yané et al. 2005; Moura et al. 2019).

978 As inferred from the phylogeny and derived interpretations here presented, the dispersal
979 events of *S. antelucanus* and *H. floridanus* to North America are independent of each other.
980 This means that the number of northward intercontinental dispersal events of pampatheriids
981 during the late Cenozoic actually is at least three, which in chronological order are: (1)
982 genus *Scirrotherium* (Late Miocene); (2) lineage *Plaina-Pampatherium* (Early Pliocene);
983 (3) genus *Holmesina* (undetermined Pliocene). From these events, only the latter, based on
984 the fossil record of *H. floridanus*, is included in the GABI. The remaining two events are
985 classified as part of the macroevolutionary invasion "wastebasket" called "Pre-GABI"

(literally, 'before the GABI'; Woodburne et al. 2006; Woodburne 2010; also named by Cione et al. 2015 as "ProtoGABI"). In the lineage *Plaina-Pampatherium*, it was differentiated one genus, *Pampatherium*, and at least three species (*P. mexicanum*, *P. typum* and *P. humboldtii*, being the two latter recorded in South America). Meanwhile, the northward dispersal event of *Scirrotherium* seems to give no origin to any other species different to *S. antelucanus*. Only a confirmed southward intercontinental dispersal event of the *Scirrotherium-Kraglievichia-Holmesina* clade has been well-established, i.e., that of *Holmesina* to South America in the Middle or early Late Pleistocene (Aguilar and Laurito 2009). This event probably is not part of any of the GABI phases of Woodburne (2010) but it appears to be chronologically located between the GABI 2 and 3.

As it has been shown, the study of more abundant and complete pampatheriid material preserved in Neogene geological units of northern South America, in particular, and the current Intertropical region of the Americas, in general, has the potential of provide us more complex and interesting scenarios on the evolution of this glyptodontoid family and, specifically, the genera *Scirrotherium* and *Holmesina*.

6. Conclusion

The monophyly of *Scirrotherium* has been tested through parsimony phylogenetic analyses. This taxon is recovered as paraphyletic. '*Scirrotherium*' *carinatum* forms a clade with *Kraglievichia paranensis* and, therefore, here it is proposed the new name *K. carinatum* comb. nov. The remaining referred species to *Scirrotherium*, *S. hondaensis* and *S. antelucanus*, are designed in aphyly. The taxonomic validity of *Scirrotherium*, as defined

here, is maintained from diagnostic evidence. *Scirrotherium* is probably the sister taxon of *Kraglievichia*, and these two genera form the sister clade of *Holmesina*. *Scirrotherium* has occurrence from the late Early Miocene to Late Pliocene of northwestern South America (Colombia and Venezuela) and the Late Miocene of southern Central America (Costa Rica). A geographic origin of Pampatheriidae in northernmost South America is suggested from the fossil record of *Scirrotherium* and a new time-calibrated phylogeny. *Scirrotherium* also represents the earliest member of Pampatheriidae which participated in a dispersal event to North America, specifically to the ancient Central American peninsula. This dispersal event happened when the Panamanian Land Bridge was not fully formed yet. The species *S. antelucanus* lived in Central America and northern Colombia during the late Neogene. This is the first Interamerican biogeographic correlation of a Neogene land mammal with high taxonomic resolution, i.e., at the species level. The record of *S. antelucanus* in both sides of the ancient Central American Seaway is compatible with a possible re-entry event of this pampatheriid to South America. In addition, *Scirrotherium* is not probably the South American ancestor of the originally-endemic North American genus *Holmesina*. In contrast with a previous hypothesis which argues that *Holmesina* may have evolved from *Kraglievichia*, here it is suggested that there is no evidence of direct ancestral forms of *Holmesina*, although the unknown South American ancestor of *Holmesina* may be morphologically more similar to *Scirrotherium*.

Acknowledgements

I am greatly indebted to all curators and managers of the collections visited for revision of specimens during this work, especially to: Andrés Vanegas (Museo de Historia Natural La

1031 Tatacoa, Colombia), Aldo Rincón (Museo Mapuka, Universidad del Norte, Colombia),
1032 Jorge Moreno-Bernal (Museo Mapuka, Universidad del Norte), Carlos De Gracia (Museo
1033 Mapuka, Universidad del Norte), Richard C. Hulbert Jr. (Florida Museum of Natural
1034 History, USA), Kenneth Angielczyk (Field Museum, USA), Bill Simpson (Field Museum
1035 of Natural History), Patricia Holroyd (University of California Museum of Paleontology,
1036 USA) and Marcelo Reguero (Museo de La Plata, Argentina). I am also grateful to Carlos
1037 Jaramillo (Smithsonian Tropical Research Institute, Panama) and his field work team from
1038 allowing access to fossils they collected in the Department of La Guajira (Colombia).
1039 Likewise, special thanks to Antonio Tovar (University of Sucre, Colombia) by inspiration
1040 to explore the Sincelejo Formation; to my field assistants during this exploration in the
1041 Department of Sucre (Colombia), Oscar Melendrez, Angel Cruz and Juan Pacheco. I would
1042 like to thank César Laurito (Instituto Nacional de Aprendizaje de Costa Rica) and Edwin
1043 Cadena (Universidad del Rosario, Colombia) for providing photos of osteoderms of the
1044 species *S. antelucanus* and one photo of outcrops of the Castilletes Formation, respectively.
1045 This work would not have been possible without logistic support and encourage by Alba
1046 Lara, Carolay Jiménez and Mónica Montalvo. An anonymous reviewer provided comments
1047 that made it possible to improve the manuscript. Financial assistance for this project was
1048 provided by several institutions/agencies: CONICET (Internal Doctoral Fellowship); Field
1049 Museum of Natural History (Science Visiting Scholarship); Florida Museum of Natural
1050 History (International Travel Grant); University of California Museum of Paleontology
1051 (Welles Fund); and The Paleontological Society (PalSIRP-Sepkoski Grant).

1052

1053 **Data archiving statement**

Data for this study are available in the Dryad Digital Repository: [Intentionally blank]

The nomenclatural acts contained in this work are registered in ZooBank:

LSID. urn:lsid:zoobank.org:act:313358B5-3B1F-4902-8C2E-BB07CFCBEE18

LSID. urn:lsid:zoobank.org:act:E3B83181-91D6-44C8-90C0-BBAACEC2CDEE

LSID. urn:lsid:zoobank.org:act:225CD304-3B63-4B55-B8B8-33B46C90A194

LSID. urn:lsid:zoobank.org:act:92C8B169-4F79-467E-B951-EF1DE6E327B1

References

Aguilar, D.H. Laurito, C.A., 2009. El armadillo gigante (Mammalia, Xenarthra, Pampatheriidae) del río Tomayate, Blancano tardío-Irvingtoniano temprano, El Salvador, América Central. Revista Geológica de América Central 41, 25–36. doi:10.15517/rgac.v0i41.4176

Aguilar, T., Acevedo, B., Ulloa, A., 2010. Paleontología de una sección del río Corredores, Formación Curré, Mioceno, Costa Rica. Revista Geológica de América Central 42, 43–75. doi:10.15517/rgac.v0i42.4170

Alfaro, E., Holz, M., 2014. Review of the chronostratigraphic charts in the Sinú-San Jacinto Basin based on new seismic stratigraphic interpretations. Journal of South American Earth Sciences 56, 139–169. doi:10.1016/j.jsames.2014.09.004

1072 Alvarado, G.E., Barquero, R., Taylor, W., López, A., Cerdas, A., Murillo, J., 2009.
1073 Geología de la hoja general, Costa Rica. Revista Geológica de América Central 40,
1074 97–107. doi:0.15517/rgac.v0i40.4189

1075 Ameghino, F., 1888. Lista de las especies de mamíferos fósiles del Mioceno superior de
1076 Monte Hermoso hasta ahora conocidas. Obras Completas y Correspondencia
1077 Científica 5, 481–496.

1078 Anderson, V.J., Horton, B.K., Saylor, J.E., Mora, A., Tesón, E., Breecker, D.O., Ketcham,
1079 R.A., 2016. Andean topographic growth and basement uplift in southern Colombia:
1080 Implications for the evolution of the Magdalena, Orinoco, and Amazon river systems.
1081 Geosphere 12, 1235–1256. doi:10.1130/GES01294.1

1082 Antoine, P.O., Abello, M.A., Adnet, S., Sierra, A.J., Baby, P., Billet, G., Boivin, M.,
1083 Calderon, Y., Candela, M.A., Chabain, J., Corfu, F., Croft, D.D., Ganerød, M.,
1084 Jaramillo, C., Klaus, S., Marivaux, L., Navarrete, R.E., Orliac, M.J., Parra, F., 2016.
1085 A 60-million-year Cenozoic history of western Amazonian ecosystems in
1086 Contamana, eastern Peru. Gondwana Research 31, 30–59.
1087 doi:10.1016/j.gr.2015.11.001

1088 Ausich, W.I., Kammer, T.W., Rhenberg, E.C.,Wright, D.F., 2015. Early phylogeny of
1089 crinoids within the pelmatozoan clade. Palaeontology 58, 937–952.
1090 doi:10.1111/pala.12204

1091 Beard, K.C., Dawson, M.R., 1999. Intercontinental dispersal of Holarctic land mammals
1092 near the Paleocene/Eocene boundary: Paleogeographic, paleoclimatic and

1093 biostratigraphic implications. Bulletin de la Société géologique de France 170, 697–
1094 706.

1095 Bengtson, P., 1988. Open nomenclature. Palaeontology 31, 223–227.

1096 Bermúdez, H.D., Alvarán, M., Grajales, J.A., Restrepo, L.C., Rosero, J.S., Guzmán, C.,
1097 Ruíz, E.C., Navarrete, R.E., Jaramillo, C., Osorno, J.F., 2009. Estratigrafía y
1098 evolución geológica de la secuencia sedimentaria del Cinturón Plegado de San
1099 Jacinto. Memorias XII Congreso Colombiano de Geología, 1–27.
1100 doi:10.13140/2.1.5072.7367

1101 Bernal-Olaya, R., Mann, P., Vargas, C.A., 2015. Earthquake, tomographic, seismic
1102 reflection, and gravity evidence for a shallowly dipping subduction zone beneath the
1103 Caribbean Margin of Northwestern Colombia, in: Bartolini, C., Mann, P. (Eds.),
1104 Petroleum Geology and Potential of the Colombian Caribbean Margin. AAPG
1105 Memoir 118, pp. 247–270. doi:10.1306/13531939M1083642

1106 Billet, G., Hautier, L., De Muizon, C. and Valentin, X., 2011. Oldest cingulate skulls
1107 provide congruence between morphological and molecular scenarios of armadillo
1108 evolution. Proceedings of the Royal Society of London B, Biological Sciences 278,
1109 2791–2797. doi:0.1098/rspb.2010.2443

1110 Bloch, J.I., Woodruff, E.D., Wood, A.R., Rincon, A.F., Harrington, A.R., Morgan, G.S.,
1111 Foster, D.A., Montes, C., Jaramillo, C.A., Jud, N.A., Jones, D.S., MacFadden, B.J.,
1112 2016. First North American fossil monkey and early Miocene tropical biotic
1113 interchange. Nature 533, 243–258. doi:10.1038/nature17415

1114 Bowen, G.J., Clyde, W.C., Koch, P.L., Ting, S., Alroy, J., Tsubamoto, T., Wang, Y., Wang,
1115 Y., 2002. Mammalian dispersal at the Paleocene/Eocene boundary. Science 295,
1116 2062–2065. doi:10.1126/science.1068700

1117 Brandoni, D., Ruiz, L.G.,Bucher, J., 2019. Evolutive Implications of *Megathericulus*
1118 *patagonicus* (Xenarthra, Megatheriinae) from the Miocene of Patagonia Argentina.
1119 Journal of Mammalian Evolution, 1–16. doi:10.1007/s10914-019-09469-6

1120 Carlini, A.A., Zurita, A.E., Scillato-Yané, G.J., Sánchez, R., Aguilera, O.A., 2008. New
1121 Glyptodont from the Codore Formation (Pliocene), Falcón State, Venezuela, its
1122 relationship with the *Asterostemma* problem, and the paleobiogeography of the
1123 Glyptodontinae. Paläontologische Zeitschrift 82, 139–152. doi:10.1007/BF02988405

1124 Carrillo, J.D., Forasiepi, A., Jaramillo, C., Sánchez-Villagra, M.R., 2015. Neotropical
1125 mammal diversity and the Great American Biotic Interchange: Spatial and temporal
1126 variation in South America's fossil record. Frontiers in Genetics 5, 451, 1–11.
1127 doi:10.3389/fgene.2014.00451

1128 Carrillo-Briceño, J.D., Reyes-Cespedes, A.E., Salas-Gismondi, R., Sánchez, R., 2018. A
1129 new vertebrate continental assemblage from the Tortonian of Venezuela. Swiss
1130 Journal of Palaeontology, 1–12. doi:10.1007/s13358-018-0180-y

1131 Cartelle, C., Bohórquez, G.A., 1985. *Pampatherium paulacoutoi*, uma nova
1132 espécie de tatu gigante da Bahia, Brasil (Edentata, Dasypodidae). Revista Brasileira de
1133 Zoologia 2, 229–254. doi:10.1590/S0101-81751983000400003

1134 Cartelle, C., De Iuliis, G., 1995. *Eremotherium laurillardi*: The Panamerican late
1135 Pleistocene megatheriid sloth. Journal of Vertebrate Paleontology 15, 830–841.
1136 doi:10.1080/02724634.1995.10011265

1137 Cartelle, C., De Iuliis, G., 2006. *Eremotherium laurillardi* (Lund) (Xenarthra,
1138 Megatheriidae), the Panamerican giant ground sloth: Taxonomic aspects of the
1139 ontogeny of skull and dentition. Journal of Systematic Palaeontology 4, 199–209.
1140 doi:10.1017/S1477201905001781

1141 Cartelle, C., De Iuliis, G., Pujos, F., 2015. *Eremotherium laurillardi* (Lund, 1842)
1142 (Xenarthra, Megatheriinae) is the only valid megatheriine sloth species in the
1143 Pleistocene of intertropical Brazil: A response to Faure et al., 2014. Comptes Rendus
1144 Palevol 14, 15–23. doi:10.1016/j.crpv.2014.09.002

1145 Castellanos, A., 1937. Anotaciones sobre la línea filogenética de clamiterios. Serie
1146 Técnico-Científica de la Facultad de Ciencias Matemáticas, Físico-Químicas y
1147 Naturales 8, 1–35. Rosario, Argentina.

1148 Cione, A., Gasparini, G., Soibelzon, E., Soibelzon, L., Tonni, E., 2015. The Great
1149 American Biotic Interchange. A South American perspective. Springer Briefs in
1150 Earth System Sciences. South America and the Southern Hemisphere, Amsterdam,
1151 Netherlands. doi:10.1007/978-94-017-9792-4

1152 Coates, A.G., Stallard, R.F., 2013. How old is the Isthmus of Panama? Bulletin of Marine
1153 Science 89, 801–813. doi:10.5343/bms.2012.1076

1154 Cortes, J.E., Aguilera, R., Wilches, O., Osorno, J.F., Cortes, S.I., 2018. Organic
1155 geochemical insights from oil seeps, tars, rocks, and mud volcanoes on the petroleum

systems of the Sinú-San Jacinto basin, Northwestern Colombia. Journal of South American Earth Sciences 86, 318–341. doi: 10.1016/j.jsames.2018.06.007

Cozzuol, M.A., 2006. The Acre vertebrate fauna: age, diversity, and geography. Journal of South American Earth Sciences 21, 185–203. doi:10.1016/j.jsames.2006.03.005

Croft, D.A. 2007., The Middle Miocene (Laventan) Quebrada Honda fauna, southern Bolivia and a description of its notoungulates. Palaeontology 50, 277–303. doi:10.1111/j.1475-4983.2006.00610.x

De Iuliis, G., Edmund, A.G., 2002. *Vassallia maxima* Castellanos, 1946 (Mammalia: Xenarthra: Pampatheriidae), from Puerta del Corral Quemado (late Miocene to early Pliocene), Catamarca Province, Argentina. Smithsonian Contributions to Paleobiology 93, 49–64.

Delsuc, F., Superina, M., Tilak, M.K., Douzery, E.J., Hassanin, A., 2012. Molecular phylogenetics unveils the ancient evolutionary origins of the enigmatic fairy armadillos. Molecular Phylogenetics and Evolution 62, 673–680. doi:10.1016/j.ympev.2011.11.008

Ebach, M.C., Williams, D.M., 2010. Aphyly: a systematic designation for a taxonomic problem. Evolutionary biology, 37 (2-3), 123–127. doi:10.1007/s11692-010-9084-5

Edmund, A.G., 1985. The armor of fossil giant Armadillos (Pampatheriidae, Xenarthra, Mammalia). Texas Memorial Museum, Pearce-Sellards-Series 40, 1–20.

Edmund, A.G., 1987. Evolution of the Genus *Holmesina* (Pampatheriidae, Mammalia) in Florida, with Remarks on Taxonomy and Distribution. Texas Memorial Museum, Pearce-Sellards-Series 45, 1–20.

1178 Edmund, A.G., Theodor, J., 1997. A new giant Armadillo, in: Kay, R.F. Cifelli, R.L., Flynn
1179 J.J., Madden, R. (Eds.), Vertebrate Paleontology of the Miocene Fauna of La Venta,
1180 Colombia. Smithsonian Institution Press, Washington, pp. 227–232.

1181 Fernícola, J.C., 2008. Nuevos aportes para la sistemática de los Glyptodontia Ameghino
1182 1889 (Mammalia, Xenarthra, Cingulata). Ameghiniana, 45, 553–574.

1183 Flinch, J.F., 2003. Structural evolution of the Sinú-Lower Magdalena area (northern
1184 Colombia), in: Bartolini, C., Buffler, R.T., Blickwede, J. (Eds.), The Circum-Gulf of
1185 Mexico and the Caribbean: Hydrocarbon Habitats, Basin Formation, and Plate
1186 Tectonics, AAPG Memoir 79, pp. 776–796.

1187 Flynn J.J., Guerrero, J., Swisher, C.C., III. 1997. Geochronology of the Honda Group, in:
1188 Kay, R.F. Cifelli, R.L., Flynn J.J., Madden, R. (Eds.), Vertebrate Paleontology of the
1189 Miocene Fauna of La Venta, Colombia. Smithsonian Institution Press, Washington,
1190 pp. 44–59.

1191 Gaudin, T.J., 2004. Phylogenetic relationships among sloths (Mammalia, Xenarthra,
1192 Tardigrada): The craniodental evidence. Zoological Journal of the Linnean Society
1193 140, 255–305. doi:10.1111/j.1096-3642.2003.00100.x

1194 Gaudin, T.J., Wible, J.R., 2006. The phylogeny of living and extinct armadillos
1195 (Mammalia, Xenarthra, Cingulata): A craniodental analysis, in: Carrano, M.T.,
1196 Gaudin, T. J., Blob, R.W., Wible, J.R. (Eds.), Amniote Paleobiology: Perspectives
1197 on the Evolution of Mammals, Birds and Reptiles. University of Chicago Press,
1198 Chicago, pp. 153–198.

1199 Gaudin, T.J., Lyon, L.M., 2017. Cranial osteology of the pampathere *Holmesina floridanus*
1200 (Xenarthra: Cingulata; Blancan NALMA), including a description of an isolated
1201 petrosal bone. PeerJ 5, e4022. doi:10.7717/peerj.4022

1202 Góis, F. 2005. Estudo descritivo e geométrico dos Cingulata (Mammalia, Xenarthra) do
1203 Neógeno e Quaternário da Amazônia Sul-Ocidental. Bachelor thesis, Universidade
1204 Federal de Rondônia (unpubl.).

1205 Góis, F. 2013. Análisis morfológico y afinidades de los Pampatheriidae (Mammalia,
1206 Xenarthra). PhD thesis, Universidad Nacional de La Plata (unpubl.).

1207 Góis, F., Scillato-Yané, G.J., Carlini, A.A., Ubilla, M., 2012. Una nueva especie de
1208 *Holmesina* Simpson (Xenarthra, Cingulata, Pampatheriidae) del Pleistoceno de
1209 Rondônia, sudoeste de la Amazonia, Brasil. Revista Brasileira de Paleontologia 15,
1210 211–227.doi: 10.4072/rbp.2012.2.09

1211 Góis, F., Scillato-Yané, G.J., Carlini, A.A., Guilherme, E., 2013. A new species of
1212 *Scirrotherium* Edmund and Theodor, 1997 (Xenarthra, Cingulata, Pampatheriidae)
1213 from the late Miocene of South America. Alcheringa: An Australasian Journal of
1214 Palaeontology 37, 177–188. doi: 10.1080/03115518.2013.733510

1215 Góis, F., Ruiz, L.R., Scillato-Yané, G.J., Soibelzon, E., 2015. A peculiar new
1216 Pampatheriidae (Mammalia: Xenarthra: Cingulata) from the Pleistocene of Argentina
1217 and comments on Pampatheriidae diversity. PloS One 10, e0128296.
1218 doi:10.1371/journal.pone.0128296

1219 Góis, F., Nascimento, E.R., Porto, A.S., Holanda, E.C., Cozzuol, M.A., 2004. Ocorrências
1220 de Cingulata dos gêneros *Kraglievichia* e *Holmesina* do Terciário e Quaternário da
1221 Amazônia Sul-Ocidental. Ameghiniana 49, 41.

1222 Guerrero, J. 1997. Stratigraphy and sedimentary environments of the Honda Group in the
1223 La Venta area. Miocene uplift of the Colombian Andes, in Kay, R.F., Cifelli, R.L.,
1224 Flynn, J.J., Madden, R. (Eds.), Vertebrate Paleontology of the Miocene Fauna of La
1225 Venta, Colombia. Smithsonian Institution Press, Washington, pp. 15–43.

1226 Goloboff, P.A., 2014. Extended implied weighting. Cladistics 30, 260–272.
1227 doi:10.1111/cla.12047

1228 Goloboff, P.A., Torres, A., Arias, J.S., 2018. Weighted parsimony outperforms other
1229 methods of phylogenetic inference under models appropriate for morphology.
1230 Cladistics 34, 407–437. doi:10.1111/cla.12205

1231 Goloboff, P.A., Carpenter, J.M., Salvador Arias, J., Miranda Esquivel, D.R., 2008.
1232 Weighting against homoplasy improves phylogenetic analysis of morphological data
1233 sets. Cladistics 24, 758–773. doi:10.1111/j.1096-0031.2008.00209.x

1234 Hoffstetter, R., 1952. Les mammifères pleistocenes de la République de l'Équateur.
1235 Mémoires Societé Géologique de France 66, 1–391.

1236 Jaramillo, C., 2018. Evolution of the Isthmus of Panama: Biological, paleoceanographic,
1237 and paleoclimatological implications, in: Hoorn, C., Antonelli, A. (Eds.), Mountains,
1238 climate and biodiversity. John Wiley and Sons, Oxford, pp. 323–338.

1239 Jaramillo, C., Romero, I., D'Apolito, C., Bayona, G., Duarte, E., Louwye, S., Escobar, J.,
1240 Luque, J., Carrillo-Briceño, J.D., Zapata, V., Mora, A., Schouten, S., Zavada, M.,

1241 Harrington, G., Wesseling, F.P., 2017. Miocene flooding events of western
1242 Amazonia. Science advances 3, e1601693. doi:10.1126/sciadv.1601693

1243 Kerber, L., Negri, F.R., Ribeiro, A.M., Nasif, N., Souza-Filho, J.P., Ferigolo, J., 2017.
1244 Tropical fossil caviomorph rodents from the southwestern Brazilian Amazonia in the
1245 context of the South American faunas: Systematics, biochronology, and
1246 paleobiogeography. Journal of Mammalian Evolution 24, 57–70.
1247 doi:10.1007/s10914-016-9340-2

1248 Kolarsky, R.A., Mann, P., Montero, W., 1995. Island arc response to shallow subduction of
1249 the Cocos Ridge, Costa Rica. Special papers of the Geological Society of America
1250 295, 235–262. doi:10.1130/SPE295-p235

1251 Latrubesse, E.M., Cozzuol, M.A., Silva-Caminha, S.A., Rigsby, C.A., Absy, M.L.,
1252 Jaramillo, C., 2010. The late Miocene paleogeography of the Amazon Basin and the
1253 evolution of the Amazon River system. Earth-Science Reviews 99, 99–124.
1254 doi:10.1016/j.earscirev.2010.02.005

1255 Laurito, C.A., Valerio, A.L., 2013. *Scirrotherium antelucanus*, una nueva especie de
1256 Pampatheriidae (Mammalia, Xenarthra, Cingulata) del Mioceno Superior de Costa
1257 Rica, América Central. Revista Geológica de América Central 49, 45–62.
1258 doi:10.15517/rgac.v0i49.13101

1259 Leidy, J., 1889. Fossil Vertebrates from Florida. Proceedings of the Academy of Natural
1260 Sciences of Philadelphia 41, 96-97.

1261 Lowery, B.J., 1982. Sedimentology and tectonic implications of the Middle to Upper
1262 Miocene Curré Formation. M.S. thesis, Louisiana State University (unpub.).

1263 Lund, P., 1839. Blik paa Braziliens Dyreverden for Sidste Jordomvaeltning. Anden
1264 Afhandling: Pattedyrene. Det Kongelige Danske Videnskabernes
1265 SelskbasNaturvidenskabelige og Mathematiske Afhandlinger 8, 61–44.

1266 Lund, P., 1842. Blik paa Braziliens Dyreverden for Sidste Jordomvaeltning.
1267 TredieAfhandling: Forsaettelse af Pattedyrene. Det Kongelige Danske
1268 Videnskabernes SelskbasNaturvidenskabelige og Mathematiske Afhandlinger 8, 217–
1269 272.

1270 MacFadden, B.J., 2006. Extinct mammalian biodiversity of the ancient New World tropics.
1271 Trends in Ecology and Evolution 21, 157–165. doi:10.1016/j.tree.2005.12.003

1272 Maddison, W.P., Maddison, D.R., 2010. Mesquite: a modular system for evolutionary
1273 analysis. Version 2.73. [http://mesquiteproject.org]

1274 Martinelli, A.G., Ferraz, P.F., Cunha, G.C., Cunha, I.C., De Souza Carvalho, I., Ribeiro, L.
1275 C.B., Macedo Neto, F., Lourencini Cavellani, C., Antunes Teixeira, V.P., Da Fonseca
1276 Ferraz, M.L., 2012. First record of *Eremotherium laurillardi* (Lund, 1842)
1277 (Mammalia, Xenarthra, Megatheriidae) in the Quaternary of Uberaba, Triângulo
1278 Mineiro (Minas Gerais State), Brazil. Journal of South American Earth Sciences, 37,
1279 202–207. doi: 10.1016/j.jsames.2012.03.006

1280 McDonald, H.G., Lundelius, E.L., Jr., 2009. The giant ground sloth *Eremotherium*
1281 *laurillardi* (Xenarthra, Megatheriidae), in: Albright, L.B. III (Ed.), Papers on
1282 geology, vertebrate paleontology, and biostratigraphy in honor of Michael O.
1283 Woodburne, Bulletin 65, Texas, pp. 407–421.

1284 McKenna, M.C., Bell, S.K., 1997. Classification of Mammals Above the Species Level.
1285 Columbia University Press, New York.

1286 Moreno, E. P., Mercerat, A., 1891. Exploración arqueológica de la provincia de Catamarca:
1287 Paleontología. Revista del Museo de La Plata, 1: 222–236.

1288 Moreno, F., Hendy, A. J.W., Quiroz, L., Hoyos, N., Jones, D.S., Zapata, V., Zapata, S.,
1289 Ballen, G.A., Cadena, E., Cárdenas, A.L., Carrillo-Briceño, J.D., Carrillo, J.D.,
1290 Delgado-Sierra, D., Escobar, J., Martínez, J.I., Martínez, C., Montes, C., Moreno, J.,
1291 Pérez, N., Sánchez, R., Suárez, C., Vallejo-Pareja, M.C., Jaramillo, C., 2015. Revised
1292 stratigraphy of Neogene strata in the Cocinetas basin, La Guajira, Colombia. Swiss
1293 Journal of Palaeontology 134, 5–43. doi: 10.1007/s13358-015-0071-4

1294 Obando, L.G., 2011. Stratigraphy and tectonic of northeast part of Dota quadrangle (1:
1295 50,000), Costa Rica. Revista Geológica de América Central 44, 71–82.

1296 O'dea, A., Lessios, H.A., Coates, A.G., Eytan, R.I., Restrepo-Moreno, S.A., Cione, A.L.,
1297 Collins, L.S., De Queiroz, A., Farris, D.W., Norris, R.D., Stallard, R.F., Woodburne,
1298 M.O., Aguilera, O., Aubry, M-P., Berggren, W.A., Budd, A.F., Cozzuol, M.A.,
1299 Coppard, S.E., Duque-Caro, H., Finnegan, S., Gasparini, G.M., Grossman, E.L.,
1300 Jhonson K.G., Lloyd, D.K, Knowlton N., Leigh E.G., Leonard-Pingel J.S., Marko,
1301 P.B., Pyenson, N.D., Rachello-Dolmen, P.G., Soibelzon, E., Soibelzon, L., Todd,
1302 J.A., Vermeij, G.J., Jackson, J.B.C., 2016. Formation of the Isthmus of Panama.
1303 Science advances 2, e1600883. doi: 10.1126/sciadv.1600883

1304 Ortiz-Jaureguizar, E., Cladera, G.A., 2006. Paleoenvironmental evolution of southern South
1305 America during the Cenozoic. Journal of Arid Environments 66, 498–532. doi:
1306 10.1016/j.jaridenv.2006.01.007

1307 Patterson, B., Pascual, R., 1968. The fossil mammal fauna of South America. The Quarterly
1308 Review of Biology 43, 409–451.

1309 Ribeiro, A.M., Madden, R.H., Negri, F.R., Kerber, L., Hsiou, A.S., Rodrigues, K.A., 2013.
1310 Mamíferos fósiles y biocronología en el suroeste de la Amazonia, Brasil, in:
1311 Brandoni, D., Noriega, J.I. (Eds.), El Neógeno de la Mesopotamia argentina.
1312 Asociación Paleontológica Argentina, Publicación Especial 14, Buenos Aires, pp.
1313 207–221.

1314 Rincón, A.D., Solórzano, A., Benammi, M., Vignaud, P., McDonald, H.G., 2014.
1315 Chronology and geology of an Early Miocene mammalian assemblage in North of
1316 South America, from Cerro La Cruz (Castillo Formation), Lara State, Venezuela:
1317 Implications in the changing course of Orinoco River hypothesis. Andean geology
1318 41, 507–528. doi: 10.5027/andgeoV41n3-a02

1319 Rincón, A.D., Solórzano, A., Macsotay, O., McDonald, H.G., Núñez-Flores, M., 2016. A
1320 new Miocene vertebrate assemblage from the Río Yuca Formation (Venezuela) and
1321 the northernmost record of typical Miocene mammals of high latitude (Patagonian)
1322 affinities in South America. Geobios 49, 395–405. doi:10.1016/j.geobios.2016.06.005

1323 Rivier, F., 1985. Sección geológica del Pacífico al Atlántico a través de Costa Rica. Revista
1324 Geológica de América Central 2, 22–32. doi:10.15517/rgac.v0i02.10480

1325 Robertson, J.S., 1976. Latest Pliocene mammals from Haile XV A, Alachua county,
1326 Florida. Bulletin of the Florida State Museum, Biological Sciences 20, 111–186.

1327 Salas-Gismondi, R., Flynn, J.J., Baby, P., Tejada-Lara, J.V., Wesselingh, F.P., Antoine, P.
1328 O., 2015. A Miocene hyperdiverse crocodylian community reveals peculiar trophic
1329 dynamics in proto-Amazonian mega-wetlands. Proceedings of the Royal Society B:
1330 Biological Sciences 282, 20142490. doi: 10.1098/rspb.2014.2490

1331 Sánchez-Villagra, M.R., 2012. Embryos in Deep Time: The Rock Record of Biological
1332 Development. University of California Press, Berkeley.

1333 Schmidt, D.N., 2007. The closure history of the Panama Isthmus: Evidence from isotopes
1334 and fossils to models and molecules, in: Williams, M., Haywood, A.M., Gregory J.F.,
1335 Schmidt, D.N. (Eds.), Deep time perspectives on climate change – marrying the
1336 signal from computer models and biological proxies. Geological Society of London,
1337 London, pp. 427–442.

1338 Scillato-Yané, G.J., Carlini, A.A., Tonni, E.P., Noriega, J.I., 2005. Paleobiogeography of
1339 the late Pleistocene pampatheres of South America. Journal of South American Earth
1340 Sciences 20, 131–138. doi:10.1016/j.jsames.2005.06.012

1341 Scillato-Yané, G.J., Góis, F., Zurita, A.E., Carlini A.A., González Ruiz, L.R., Krmpotic,
1342 C.M., Oliva, C., Zamorano, M. 2013. Los Cingulata (Mammalia, Xenarthra) del
1343 'Conglomerado Osífero' (Mioceno tardío) de la Formación Ituzaingó de Entre Ríos,
1344 Argentina, in: Brandoni, D., Noriega, J.I. (Eds.), El Neógeno de la Mesopotamia
1345 argentina. Asociación Paleontológica Argentina, Publicación Especial 14, Buenos
1346 Aires, pp. 118–134.

1347 Sigovini, M., Keppel, E., Tagliapietra, D., 2016. Open Nomenclature in the biodiversity
1348 era. Methods in Ecology and Evolution 7, 1217–1225. doi:10.1111/2041-210X.12594

1349 Simpson, G.G., 1930. *Holmesina septentrionalis*, extinct giant armadillo of Florida.
1350 American Museum Novitates 442, 1–10.

1351 Silva, J.C., Pardo, A., Cardona, A., Borrero, C., Flores, A., Navarette, R., Mejía, A., Ochoa,
1352 D., Osorio, J.A., Rosero, S., Arenas, A., 2012. Multi-Chronological Proxies to
1353 Timing Early Oligocene and Middle Miocene Deformation Events Along the Lower
1354 Magdalena Basin, NW Colombia. Resúmenes del XI Simposio Bolivariano-
1355 Exploración Petrolera en las Cuencas Subandinas, Asociación Colombiana de
1356 Geólogos y Geofísicos del Petróleo. Available in:
1357 [http://www.earthdoc.org/publication/publicationdetails/?publication=66175]

1358 Stirton, R.A., 1953. Vertebrate paleontology and continental stratigraphy in Colombia.
1359 Geological Society of America Bulletin 64, 603–622.

1360 Swofford, D.L., 2015. PAUP*: Phylogenetic analysis using parsimony (and other methods)
1361 (version 4.0a142).

1362 Swofford, D.L., Bell, C.D., 2017. PAUP* manual. Available at
1363 http://phylosolutions.com/paup-documentation/paupmanual.pdf.

1364 Tito, G., 2008. New remains of *Eremotherium laurillardi* (Lund, 1842) (Megatheriidae,
1365 Xenarthra) from the coastal region of Ecuador. Journal of South American Earth
1366 Sciences 26, 424–434. doi:10.1016/j.jsames.2008.05.001

1367 Villarroel, C., Clavijo, J., 2005. Los mamíferos fósiles y las edades de las sedimentitas
1368 continentales del Neógeno de la Costa Caribe Colombiana. Revista de la Academia
1369 Colombiana de Ciencias 29, 345–356.

1370 Vizcaíno, S.F., De Iuliis, G., Bargo, M.S., 1998. Skull shape, masticatory apparatus, and
1371 diet of *Vassallia* and *Holmesina* (Mammalia: Xenarthra: Pampatheriidae): When
1372 anatomy constrains destiny. Journal of Mammalian Evolution 5, 291–322. doi:
1373 10.1023/A:1020500127041

1374 Webb, S.D., 2006. The Great American Biotic Interchange: Patterns and Processes. Annals
1375 of the Missouri Botanical Garden 93, 245–258. doi: 10.3417/0026-
1376 6493(2006)93[245:TGABIP]2.0.CO;2

1377 Woodburne, M.O., 2010. The Great American Biotic Interchange: dispersals, tectonics,
1378 climate, sea level and holding pens. Journal of Mammalian Evolution 17, 245–264.
1379 doi:10.1007/s10914-010-9144-8

1380 Woodburne, M.O., Swisher, C.C. III., 1995. Land mammal high-resolution geochronology,
1381 intercontinental overland dispersals, sea level, climate and vicariance, in: Berggren,
1382 W.A., Kent, D.W., Aubry, M.-P., Hardenbol, J. (Eds.), Geochronology, Time Scales
1383 and Global Stratigraphic Correlation. SEPM Special Publication 54, pp. 335–364.

1384 Woodburne, M.O., Cione, A.L., Tonni, E.P., 2006. Central American provincialism and the
1385 Great American Biotic Interchange. Universidad Nacional Autónoma de México,
1386 Instituto de Geología y Centro de Geociencias, Publicación Especial 4, 73–101.

1387 Yuan, P.B. 1984. Stratigraphy, sedimentology and geologic evolution of eastern Terraba
1388 Trough, southwestern Costa Rica. PhD thesis, Louisiana State University (unpub.).

1389 Zurita, A.E., Scillato-Yané, G.J., Ciancio, M., Zamorano, M., González-Ruiz, L.R., 2016.
1390 Los Glyptodontidae (Mammalia, Xenarthra): Historia biogeográfica y evolutiva de un
1391 grupo particular de mamíferos acorazados. Contribuciones del MACN 6, 249–262.

Figure captions

Figure 1. Geographic and stratigraphic provenance of the newly described material of pampatheriids from the Neogene of Colombia. In the left upper corner, a map of northwesternmost South America and the location of the regions of Colombia where there are outcrops of the formations with pampatheriid specimens for this study. In the right upper corner, photos of characteristic outcrops of these formations. Below in the center, a general chronostratigraphic scheme with the position of each formation within the Neogene and two important tectonic/palaeogeographic events in northwestern South America, i.e., a major, underwater uplift of the Isthmus of Panama (Schmidt 2007) and the definitive emergence of the Panamanian Land Bridge (O'dea et al. 2016). The photo of an outcrop of the Castilletes Formation was taken by Edwin Cadena.

Figure 2. Phylogenetic results. A, strict consensus tree of the parsimony with equal weights. B, strict consensus tree of the parsimony analysis with implied weights. The numbers below nodes are bootstrap resampling frequencies. Note the difference in the phylogenetic position of *Holmesina floridanus* in the two strict consensus trees. Explanation of this difference in the *Discussion* section.

Figure 3. Fixed and (semi) mobile osteoderms of *Scirrotherium hondaensis* from the La Victoria and Villavieja Formations, Municipality of Villavieja, Department of Huila, Colombia. A–B', fixed osteoderms; C'–K', (semi) mobile osteoderms. The osteoderms G, J, K, L, W, X, Y, Z, A', B', G', I', J' and K' are associated with the catalog number VPPLT 348. The osteoderms H, U and V are associated with the catalog number VPPLT 004. The osteoderms T and D' are associated with the catalog number VPPLT 701. All the former osteoderms come from the lower and middle La Victoria Formation. The osteoderms B, C,

F, I, O, P, S, C' and F' are associated with the catalog number VPPLT 1683 - MT 18 and come from the top of the La Victoria Formation. The osteoderms A, D, E, M, N, Q, R, E' and H' are associated with the catalog number VPPLT 1683 - MT 18 and come from the lower Villavieja Formation. Scale bar equal to 20 mm.

Figure 4. Photos and anatomical line drawings of the skull VPPLT 706 of *Scirrotherium hondaensis* from the middle La Victoria Formation, Municipality of Villavieja, Department of Huila, Colombia. A–B, dorsal views; C–D, ventral views; E–F, right lateral views; D–H, left lateral views. *Abbreviations*: aof, antorbital fossa; fr, frontal; iof, infraorbital foramen; la, lacrimal; Mf1, first upper molariform; Mf9, ninth upper molariform; mx, maxilla; mxf, maxillary foramen; na, nasal; pal, palatine; pm, premaxilla. Scale bar equal to 50 mm.

Figure 5. Photos and anatomical line drawings of the left femur and right ulna VPPLT 706 of *Scirrotherium hondaensis* from the middle La Victoria Formation, Municipality of Villavieja, Department of Huila, Colombia. The epiphyses of this femoral diaphysis have been reconstructed from those with catalog number UCMP 39846. A–B, anterior views of the femur; C–D, posterior views of the femur. E–F, medial views of the ulna; G–H, lateral views of the ulna. *Abbreviations*: anc, fossa for the anconeus muscle; cp, coronoid process; fh, femoral head; gt, greater trochanter; le, lateral epicondyle; me, medial epicondyle; op, olecranon process; tn, trochlear notch; tt, third trochanter. Scale bar equal to 50 mm.

Figure 6. Photos and anatomical line drawings of a thoracic vertebra (A–B) and several anterior caudal vertebrae (C–F) VPPLT 706 of *Scirrotherium hondaensis* from the middle La Victoria Formation, Municipality of Villavieja, Department of Huila, Colombia. A–B, posterior views of the thoracic vertebra. C–D, lateral views of caudal vertebrae; E–F, dorsal views of caudal vertebrae. *Abbreviations*: az, anterior zygapophyses; mp, metapophyses;

ns, neural spine; tp, transverse processes; vb, vertebral body; vla, ventrolateral apophyses. Scale bar equal to 30 mm.

Figure 7. Photos and anatomical line drawings of the astragalus (A–D) and calcaneum (E – F) UCMP 39846 of *Scirrotherium hondaensis* from the lower (?) Villavieja Formation, Municipality of Villavieja, Department of Huila, Colombia. A–B, astragalus in plantar views; C–D, astragalus in dorsal views. E–F, calcaneum in dorsal views. *Abbreviations*: ct, calcaneal tuber; ef, ectal facet; h, head of the astragalus; lt, lateral trochlea; mt, medial trochlea; sf, sustentacular facet; st, sulcus tali. Scale bar equal to 20 mm.

Figure 8. Fixed osteoderm MUN STRI 36880 of *Scirrotherium antelucanus* from the upper Sincelejo Formation, Department of Sucre, Colombia. Scale bar equal to 20 mm.

Figure 9. Pampatheriid osteoderms from the Department of La Guajira, Colombia, referred to as aff. *Scirrotherium* (**A**, MUN STRI 16718; **E**, MUN STRI 38064; and **G,** MUN STRI 16719; all these specimens are from the Castilletes Formation and they are fixed osteoderms except the latter, which consist of an anterior fragment of a mobile osteoderm); *Scirrotherium* cf. *hondaensis* (**C**, MUN STRI 36814, a fixed osteoderm from the Castilletes Formation); and *Scirrotherium* sp. (**B**, MUN STRI 36801; **D**, MUN STRI 16158; and **F**, MUN STRI 34373; all these fixed osteoderms are from the Castilletes Formation, except the latter, which comes from the Ware Formation). Note the two well-developed rows of anterior foramina in the osteoderms MUN STRI 16718 and 38064. Scale bar equal to 20 mm.

Figure 10. Osteoderms of *Kraglievichia carinatum* comb. nov. from the Ituzaingó Formation, Province of Entre Ríos, Argentina. The holotype of this species is marked with

one single asterisk (*) and paratypes with double asterisk (**). A–J, fixed osteoderms; K–R, (semi) mobile osteoderms. **A**, MLP 69-IX-8-13AC**; **B**, MLP 70-XII-29-1**; **C**, MLP 41-XII-13-905; **D**, MLP 69-IX-8-13AF; **E**, MLP 69-IX-8-13AG; **F**, MLP 41-XII-13-414A; **G**, MLP 69-IX-8-13AN; **H**, unknown catalog number; **I**, MLP 69-IX-8-13AK; **J**, MLP 41-XII-13-414B; **K**, MLP 69-IX-8-13AS; **L**, MLP 69-IX-8-13AE**; **M**, MLP 52-X-1-36; **N**, MLP 69-IX-8-13AB*; **O**, MLP 41-XII-13-909; **P**, MLP 69-IX-8-13AW; **Q**, MLP 69-IX-8-13AQ; **R,** MLP 69-IX-8-13AY. Scale bar equal to 20 mm.

Figure 11. Hypothetical time-calibrated phylogeny of the clade *Scirrotherium* + *Kraglievichia* + *Holmesina* based on the strict consensus tree under implied weights (Fig. 2(B)). Polytomies were resolved by (1) forcing the monophyly of *S. hondaensis* and *S. antelucanus* and (2) placing the species *H. septentrionalis* and *H. occidentalis* as successively basal to the largest South American *Holmesina* species, i.e., *H. paulacoutoi* and *H. major*. Note the diversification events of the clade *Scirrotherium* + *Kraglievichia* + *Holmesina* are mainly concentrated during the Burdigalian (late Early Miocene) and Plio-Pleistocene. Likewise, note the relative long ghost lineage of *Holmesina*. Images of the pampatheriids are from *PhyloPic* (all available under public domain): top, *Pampatherium humboldtii* (http://phylopic.org/name/670230e9-4775-493c-b3ab-31718fb570a3); below, *Holmesina floridanus* (http://phylopic.org/name/73635941-ed8a-4518-aae8-70e824dbee97).

Figure 12. Geographic distributions of *Scirrotherium*, *Kraglievichia* and *Holmesina* during the Neogene and Pleistocene. The symbols (i.e., circles and triangles) should not necessarily be interpreted as single localities but as approximate areas of occurrence. This

is especially true for the Pliocene and Pleistocene epochs. Further details on the biogeography of these genera in the *Discussion* section. Scale bar equal to 2000 Km.

TABLES

Table 1. Fixed (scapular and pelvic) osteoderm measurements for taxa of interest in this study.

Taxon/Measurement	Length	Width	Thickness	References
S. hondaensis	16-35.2	17.5-27.9	3.7-6.9	This work; Góis et al. 2013
S. antelucanus	28.6-40.9	22-32.4	4.9-7.1	This work; Laurito and Valerio 2013
K. carinatum comb. nov.	20.9-33.5	17-26.1	4.1-5.9	This work; Góis et al. 2013
K. paranensis	30-45	22.5-28.3	6-11	Góis et al. 2013
H. floridanus	24.4-36.7	18.9-32.1	6-9.7	This work; Edmund 1987

Table 2. Mobile and semi-mobile osteoderm measurements for taxa of interest in this study.

Taxon/Measurement	Length	Width	Thickness	References
S. hondaensis	29.4-60	17.9-27.4	4.9-7.3	This work; Góis et al. 2013
S. antelucanus	38.2-64.6	19.4-28.9	-	Laurito and Valerio 2013
K. carinatum comb. nov.	32-54.5	17-28.9	3.9-6	This work; Góis et al. 2013
K. paranensis	60.5-70.5	25-29	7-9	Góis et al. 2013
H. floridanus	61.8-71	17.6-28.5	4.7-6.3	This work; Edmund 1987

Table 3. Selected cranial measurements for VPPLT 706 of *Scirrotherium hondaensis* and related taxa whose skulls are known.

Taxon/Measurement	GSL	NL	FL	PAL	LUR	PL	References
S. hondaensis	117.3*	~52.8	~55	-	84.1	94.3	This work
K. cf. *paranensis*	194	58	62	74	-	159	This work
*H. floridanus***	249	106.3	75	58.6	133.6	185	This work
H. septentrionalis	290	-	-	-	165	220	Góis et al. 2012

*Incomplete

**Specimen UF 191448

Table 4. Femoral measurements for *Scirrotherium hondaensis* and related taxa whose femur is known.

Measurement/Taxon	GFL	TTW	DW	References
S. hondaensis	162*	27.6	32.5	This work
K. cf. *paranensis*	164	33.7	38	This work
*H. floridanus***	195	41	47	This work
H. septentrionalis	290	70	86	Góis 2013

*Estimated from the specimens VPPLT 706 and UCMP 39846

**Specimen UF 24918

Figure 1

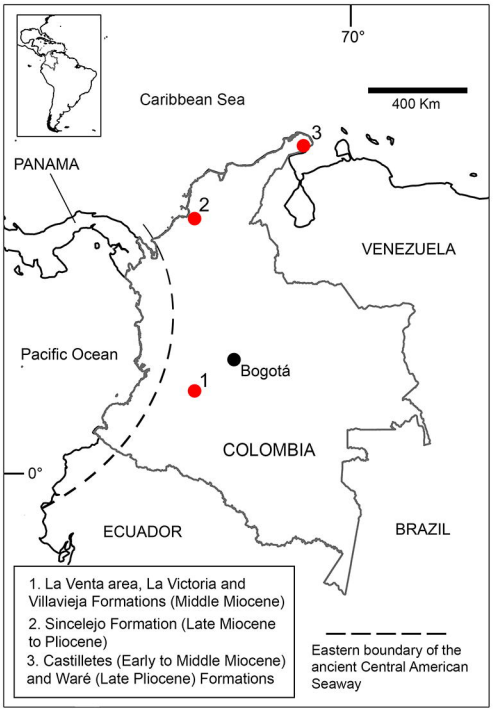

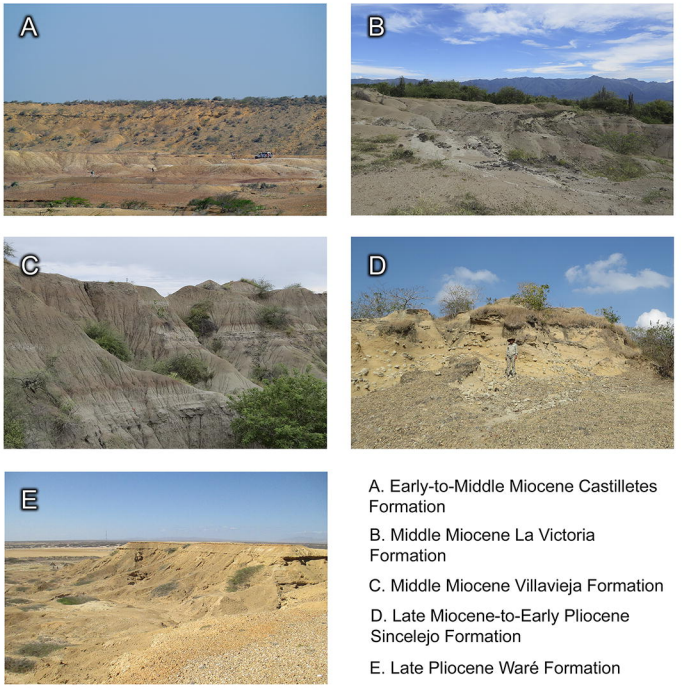

A. Early-to-Middle Miocene Castilletes Formation

B. Middle Miocene La Victoria Formation

C. Middle Miocene Villavieja Formation

D. Late Miocene-to-Early Pliocene Sincelejo Formation

E. Late Pliocene Waré Formation

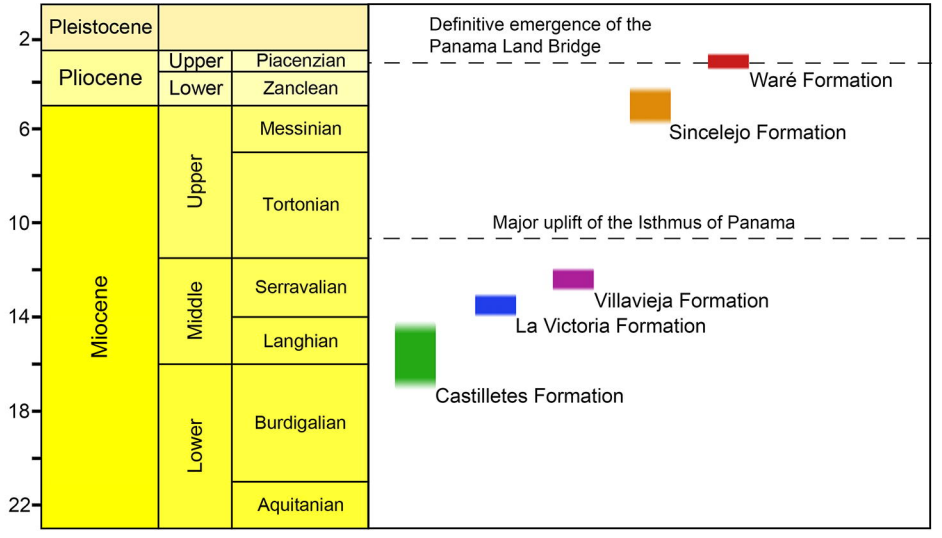

Figure 2

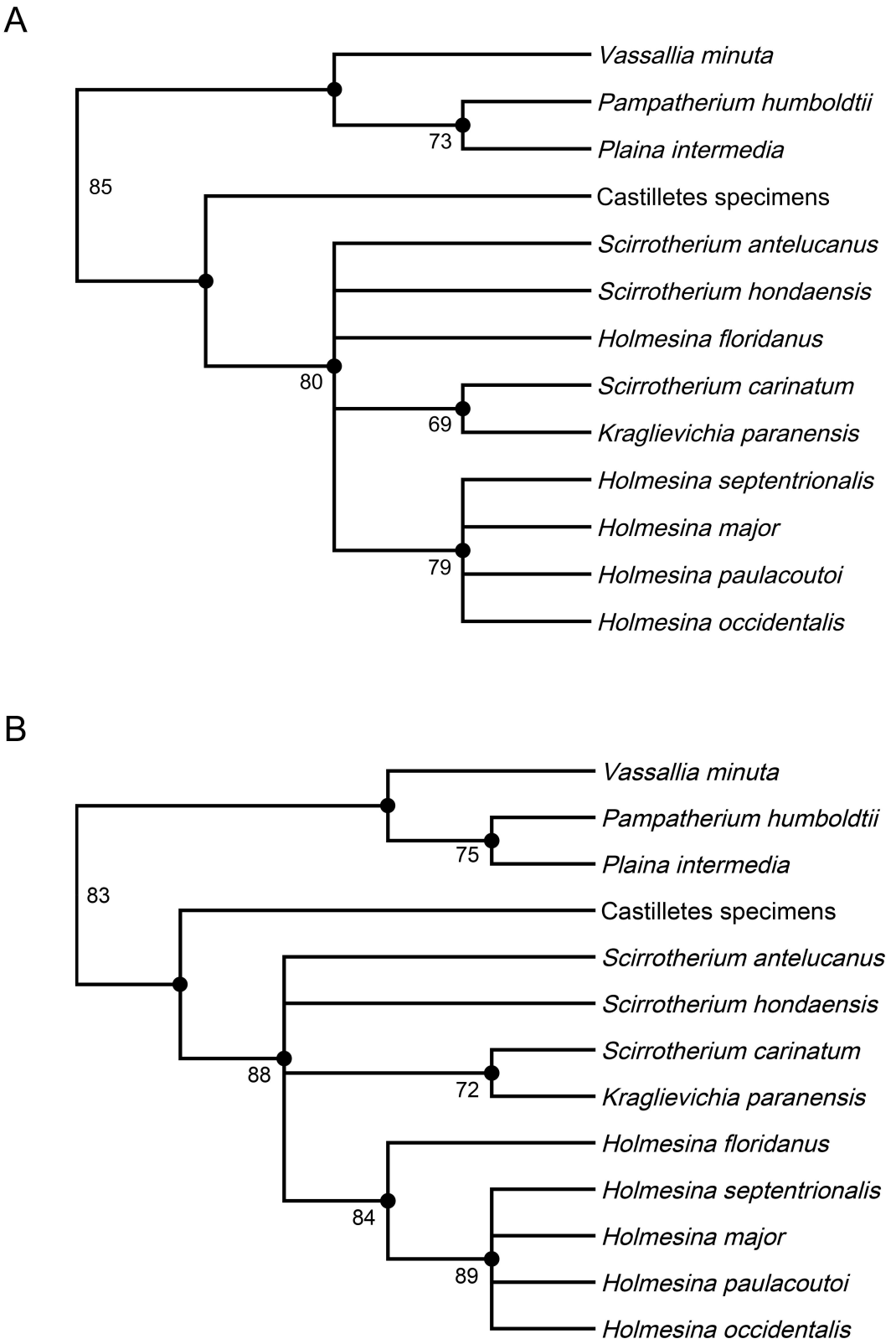
A
Vassallia minuta
Pampatherium humboldtii
Plaina intermedia
Castilletes specimens
Scirrotherium antelucanus
Scirrotherium hondaensis
Holmesina floridanus
Scirrotherium carinatum
Kraglievichia paranensis
Holmesina septentrionalis
Holmesina major
Holmesina paulacoutoi
Holmesina occidentalis
73
85
80
69
79
B
Vassallia minuta
Pampatherium humboldtii
Plaina intermedia
Castilletes specimens
Scirrotherium antelucanus
Scirrotherium hondaensis
Scirrotherium carinatum
Kraglievichia paranensis
Holmesina floridanus
Holmesina septentrionalis
Holmesina major
Holmesina paulacoutoi
Holmesina occidentalis
75
83
88
72
84
89

Figure 3

Figure 4

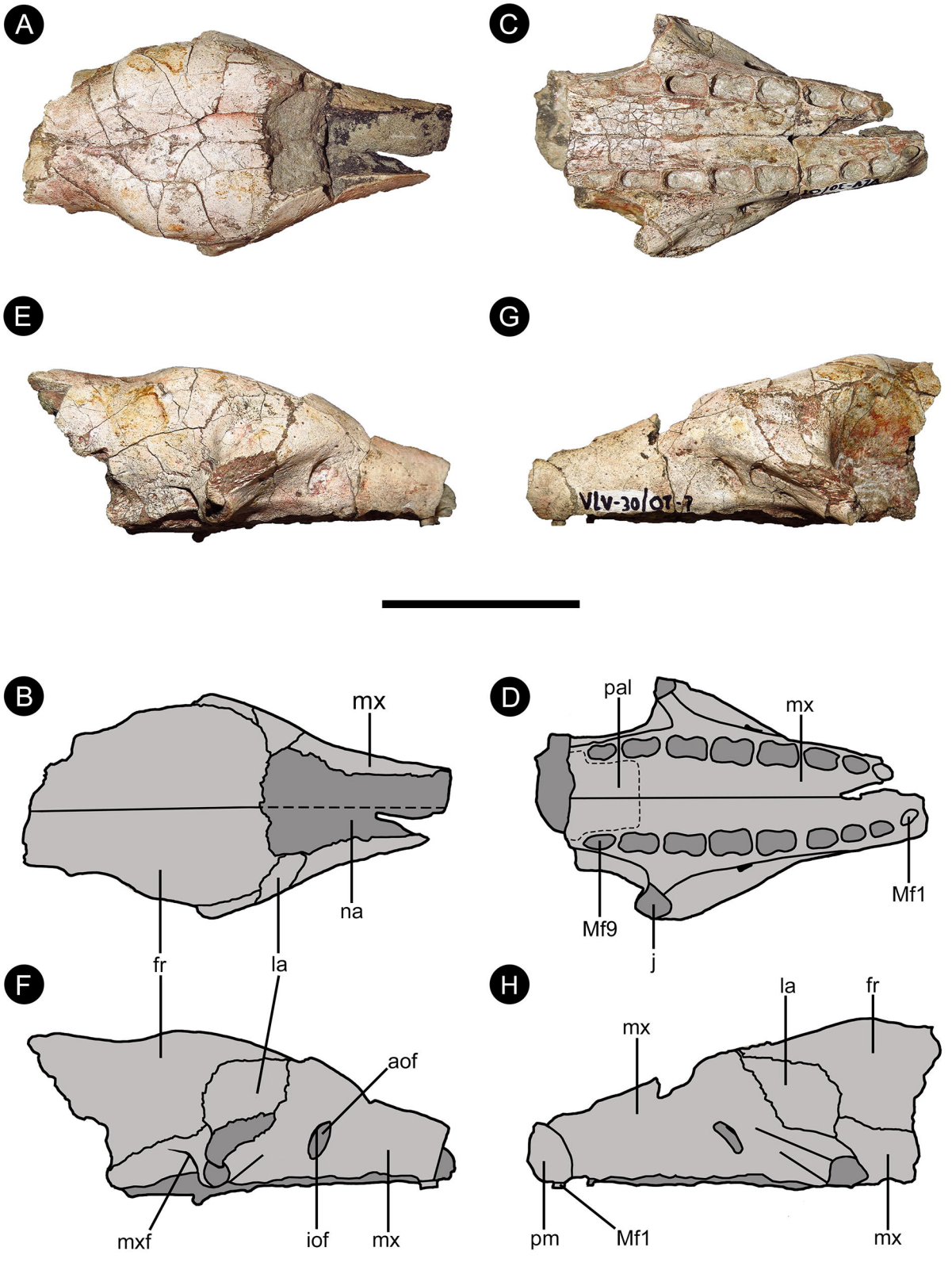
A
C
E
G
VLV-30/OT-7
B
mx
na
fr
la
D
pal
mx
Mf1
Mf9
j
F
aof
mxf
iof
mx
H
la
fr
mx
pm
Mf1
mx

Figure 5

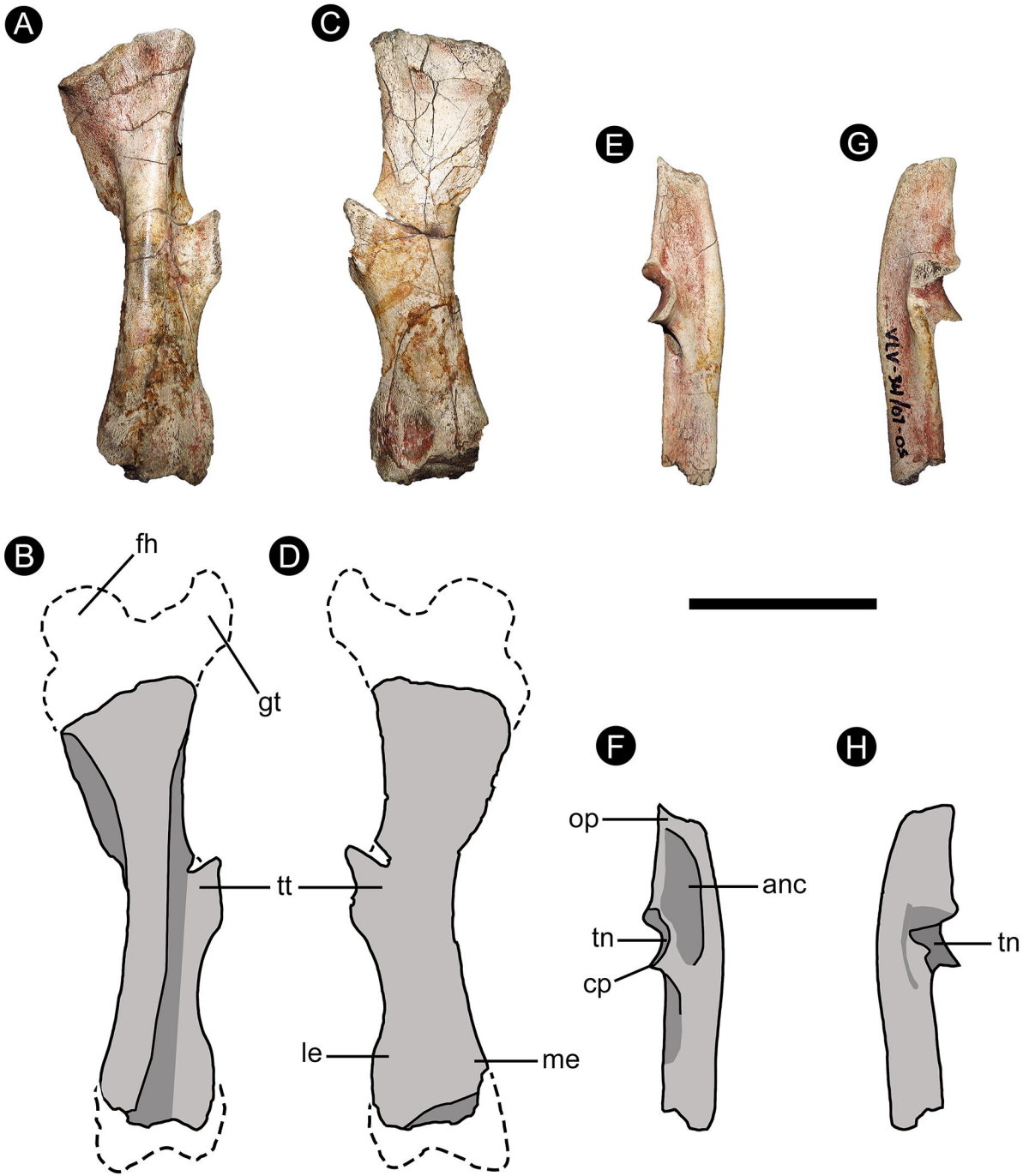

Figure 6

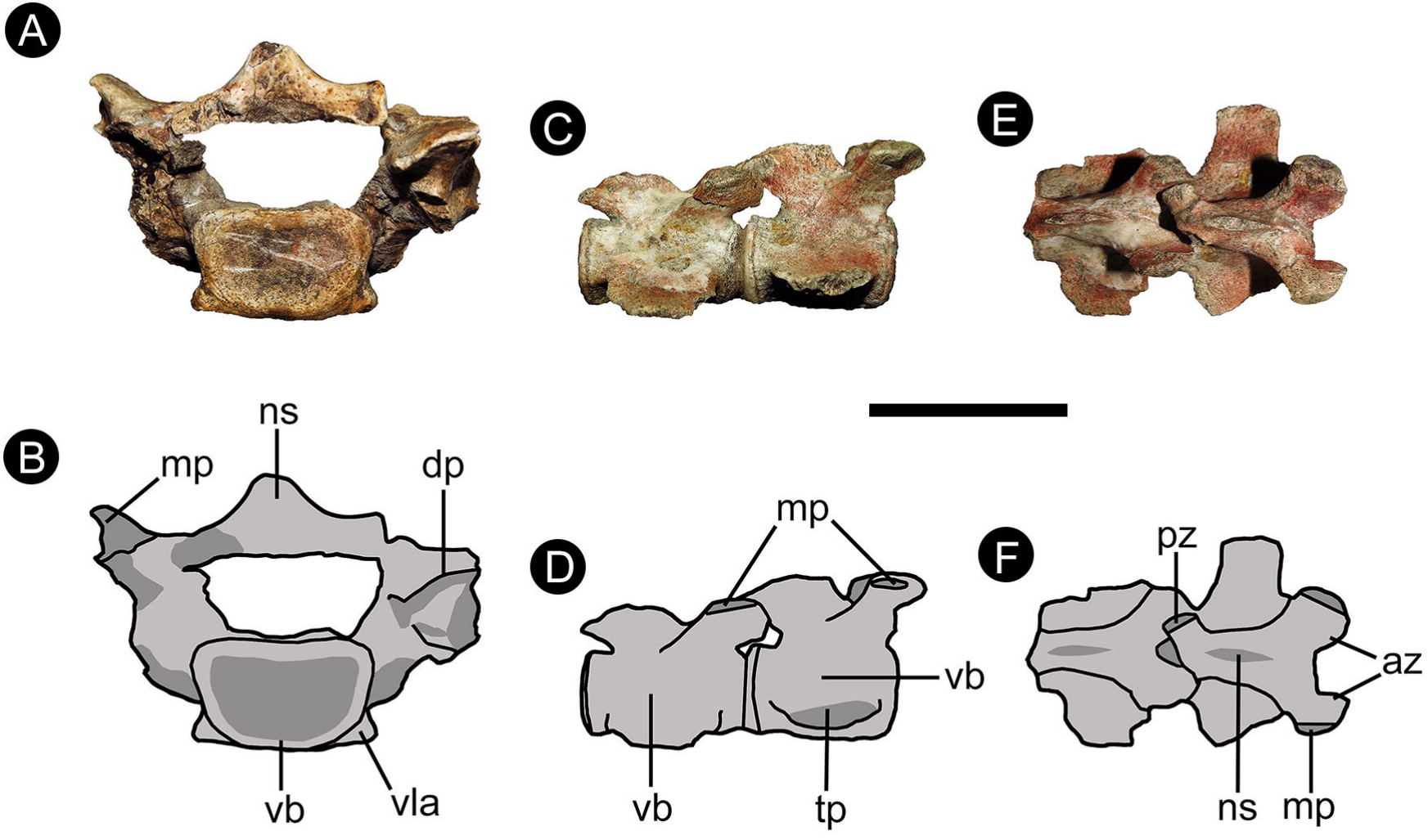

Figure 7

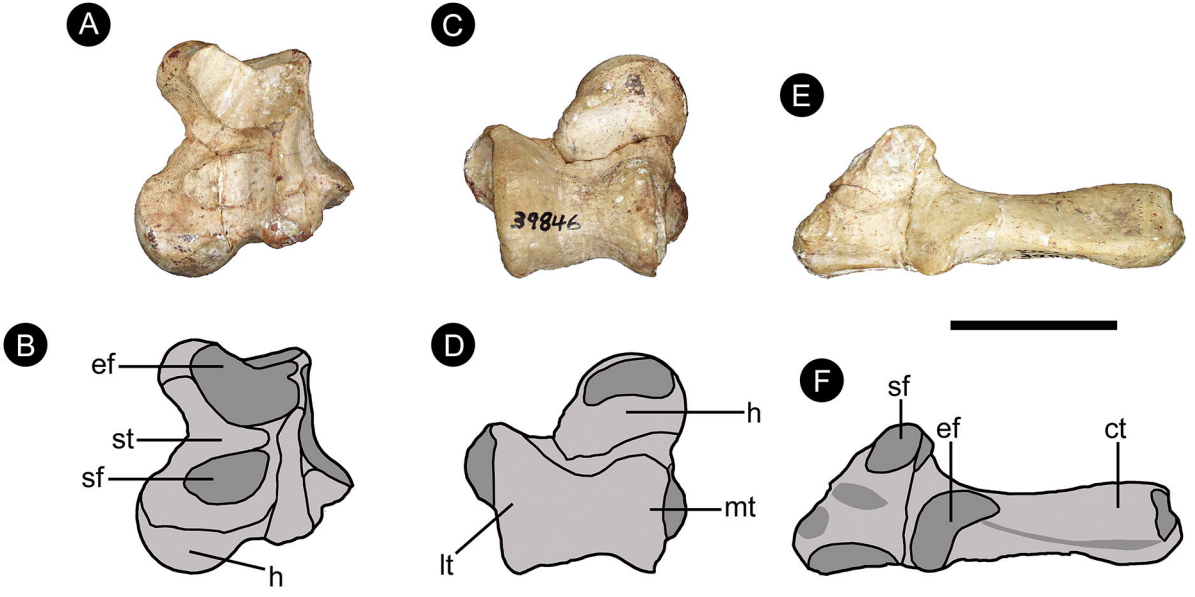

Figure 8

Figure 9

Figure 10

Figure 11

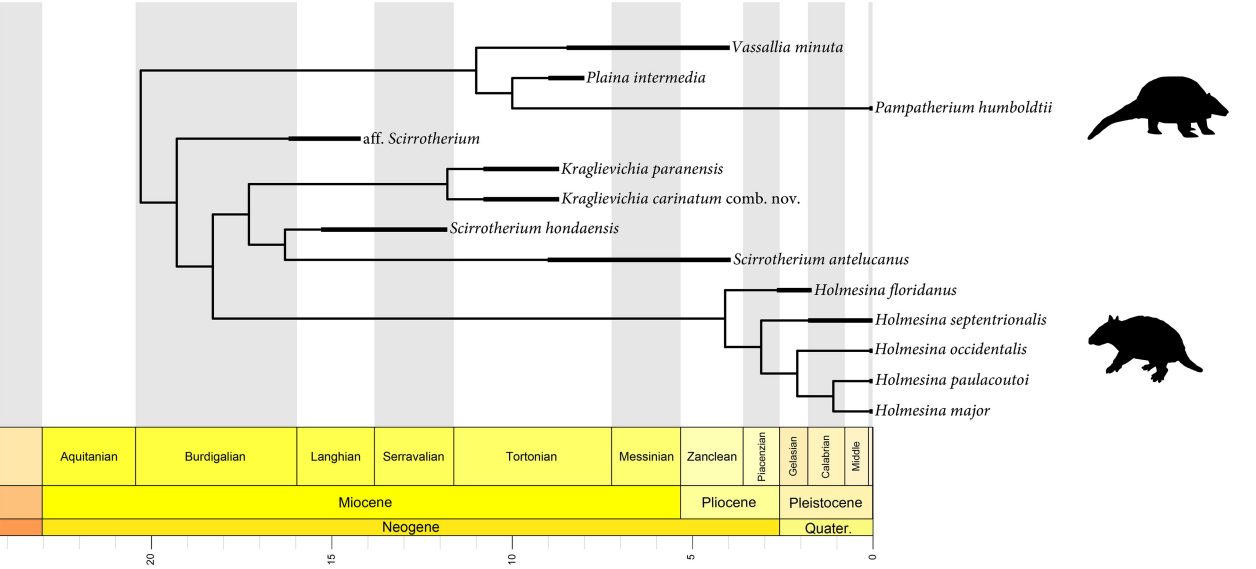
Vassallia minuta
Plaina intermedia
Pampatherium humboldtii
aff. Scirrotherium
Kraglievichia paranensis
Kraglievichia carinatum comb. nov.
Scirrotherium hondaensis
Scirrotherium antelucanus
Holmesina floridanus
Holmesina septentrionalis
Holmesina occidentalis
Holmesina paulacoutoi
Holmesina major
Aquitanian
Burdigalian
Langhian
Serravalian
Tortonian
Messinian
Zanclean
Piacenzian
Gelasian
Calabrian
Middle
Miocene
Pliocene
Pleistocene
Neogene
Quater.
20
15
10
5
0

Figure 12

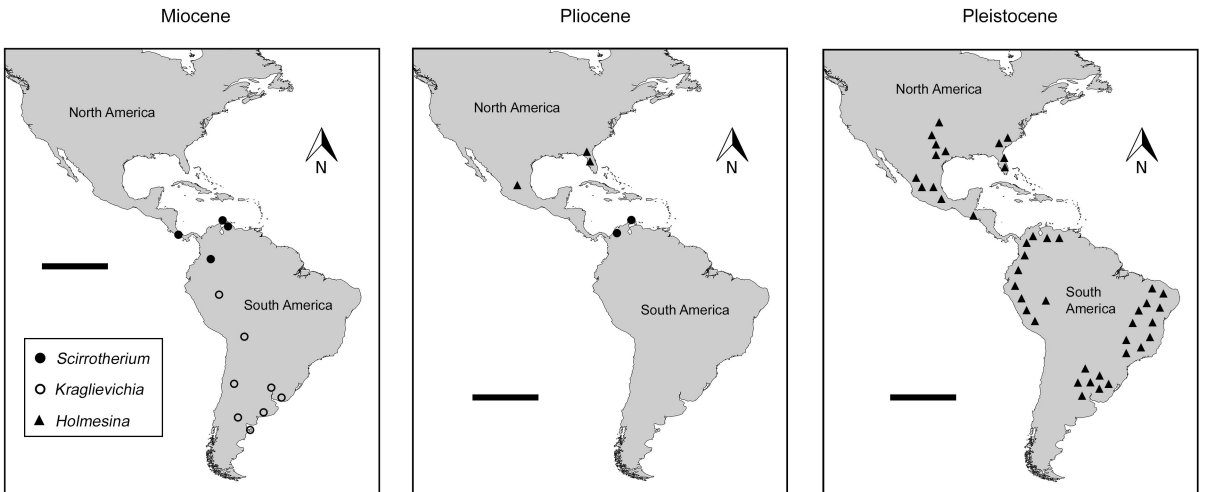
Miocene
North America
N
South America
Scirrotherium
Kraglievichia
Holmesina
Pliocene
North America
N
South America
Pleistocene
North America
N
South America